

CR 86299

N70-14840

Final Interim Technical Report

SPACE QUALIFIED CO₂ LASER

(PHASE I - DESIGN)

By Richard S. Reynolds

December 1969

Distribution of this report is provided in the interest of information exchange and should not be construed as endorsement by NASA of the material presented. Responsibility for the contents resides with the organization that prepared it.

Prepared under Contract No. NAS 12-2021
by
SYLVANIA ELECTRONIC SYSTEMS - WESTERN DIVISION
Post Office Box 188
Mountain View, California

**CASE FILE
COPY**

For

NATIONAL AERONAUTICS AND SPACE ADMINISTRATION
Electronics Research Center
Cambridge, Massachusetts

Final Interim Technical Report

SPACE QUALIFIED CO₂ LASER
(PHASE I - DESIGN)

By Richard S. Reynolds

December 1969

Prepared under Contract No. NAS 12-2021
by
SYLVANIA ELECTRONIC SYSTEMS - WESTERN DIVISION
Post Office Box 188
Mountain View, California

For
NATIONAL AERONAUTICS AND SPACE ADMINISTRATION
Electronics Research Center
Cambridge, Massachusetts

FOREWORD

This report is the Final Interim Report summarizing the work performed on Phase I (design phase) of NASA Contract NAS 12-2021 entitled "Space Qualified CO₂ Laser", covering the period 18 November 1968 to 18 September 1969. This report was prepared by the Electro-Optics Organization of Sylvania Electronic Systems - Western Division, Mountain View, California. It describes work performed in the Research and Development Department, headed by Dr. Donald E. Caddes. Mr. Richard S. Reynolds is the principal investigator on the program. Other contributors to this report are Mr. R. B. Emmons and Mr. R. Moser.

All the work performed under this contract was administered by the Chemical Physics Branch, NASA - Electronics Research Center, Cambridge, Massachusetts. Dr. Thomas E. Lawrence is the principal technical representative for the Chemical Physics Branch.

ABSTRACT

This report presents the preliminary detail design of a 1 watt, space-qualified CO₂ laser. The laser tube utilizes a beryllium oxide ceramic structure for enhanced heat removal and is conduction cooled. The tube has gallium arsenide Brewster windows so that in-cavity optical components (such as an electro-optic modulator) can be added if required. The laser head has a design weight of 5.9 lbs and measures 12 x 4 x 4 inches. The design employs an external power supply which has a design weight of 4.2 lbs and measures 2 x 4 x 9 inches. A new metal-soldering technique was developed which allows bakeable ultra-high vacuum seals to be made between the GaAs windows and the laser tube. The laser is equipped with a piezoelectric mirror transducer so that manual or automatic control of the laser frequency is possible. Experimental studies on mock-up lasers have shows that an overall efficiency of about 7% or better is possible with close attention to the detailed tube design. Continuing life studies have resulted in over 3400 hours of operating life at less than 25% reduction in initial power output. To achieve these lifetimes, a continuously-heated nickel cathode was used.

TABLE OF CONTENTS

<u>Section</u>	<u>Title</u>	<u>Page</u>
1.0	INTRODUCTION	1
2.0	GENERAL SPECIFICATIONS FOR SPACE-QUALIFIED CO ₂ LASER	3
2.1	Laser Head and Electronics Specifications	3
2.2	Qualification Test Requirements	5
2.2.1	Vibration	5
2.2.2	Shock (Launch)	5
2.2.3	Acoustical Noise	6
2.2.4	Acceleration	6
2.2.5	Temperature	6
2.2.6	Thermal Shock	7
2.2.7	Temperature - Altitude	7
2.2.8	Humidity	7
2.2.9	Electromagnetic Compatibility	7
2.2.10	Operational Life Tests	7
2.2.11	Shelf Life Tests	7
2.2.12	Beam Quality	7
2.2.13	Oxygen Atmosphere	7
2.2.14	Salt Fog Test	7
2.2.15	Explosive Atmosphere Test	7
3.0	LASER DESIGN	8
3.1	General and Summary	8
3.2	Tube Design	14
3.3	Optical Design	18
3.3.1	Gain Characteristics	18
3.3.2	Laser Bore and Mirror Design	21
3.4	Frequency Stability Considerations	25
3.4.1	Short-Term Frequency Stability	26
3.4.2	Long-Term Frequency Stability	27
3.4.3	Electronic Laser Frequency Control	31
3.5	Transducer Design	35

TABLE OF CONTENTS

<u>Section</u>	<u>Title</u>	<u>Page</u>
3.6	Power Monitor and Wavelength Identifier	40
	3.6.1 Power Monitor	40
	3.6.2 Wavelength Identifier	40
3.7	Power Supply Design	45
	3.7.1 General	45
	3.7.2 Circuit Description	47
	3.7.3 Starting Circuit	51
	3.7.4 Command Circuit	51
	3.7.5 Monitor Outputs	51
	3.7.6 Packaging	51
4.0	EXPERIMENTAL STUDIES	54
	4.1 Introduction	54
	4.2 Laser Life Tests	54
	4.2.1 General	54
	4.2.2 Life Test Station	54
	4.2.3 Description of Life Test Lasers	60
	4.2.4 Life Test Results	64
	4.3 GaAs Window Sealing Studies	72
	4.4 Beryllium Oxide Leak Rate Measurements	75
	4.4.1 Tube Leak Rate Requirement	75
	4.4.2 BeO Leak Rate Experiments	77
	4.5 Mock-up Laser Tests	79
	4.6 Electrode Fall Studies	81
5.0	MATERIALS LIST	87
6.0	SUMMARY AND CONCLUSIONS	88
7.0	REFERENCES	90
	APPENDIX A	91

LIST OF ILLUSTRATIONS

<u>Figure</u>	<u>Title</u>	<u>Page</u>
3-1	Block Diagram, Space Qualified CO ₂ Laser Design	10
3-2	Space Qualified Laser Head Assembly	12
3-3	Space Qualified Laser Tube Assembly	15
3-4	Output Power as a Function of Mirror Reflectance for a Number of Values for the Single-Pass Gain	20
3-5	Power Output vs Bore Temp. of Small CO ₂ Laser	22
3-6	Diagram of Laser Showing Elements Affecting Frequency Stability due to Temperature Drifts	28
3-7	Generation and Measurement of the Frequency Calibration Discriminant	32
3-8	Laser Frequency Control	36
3-9	Doubly Clamped Bimorph With Laser Mirror Mounted	38
3-10	Bolometer Electrical Circuit	41
3-11	Pass Band Characteristics of a Short Fabry-Perot Etalon	43
3-12	Power Supply System Block Diagram	48
3-13	Typical Simplified Circuit	49
3-14	Voltage Converter and Waveforms	50
3-15	3.5kV Current Regulated Laser Power Supply	53
4-1	Laser Life Test Station Block Diagram	55
4-2	Photograph of Life Test Facility	56
4-3	Residual Gas Analyzer	57
4-4	Calibrated Gas Sampling Valve	59
4-5	Cathode Configuration for Life Test Lasers	63
4-6	Life History of S.Q.-2 CO ₂ Laser	66
4-7	Life Test Laser, S.Q.-2	67
4-8	Life Test Laser, S.Q.-3	69
4-9	Life History of S.Q.-3 Laser Cathode Heater From Start of Life Test	70
4-10	Gallium Arsenide Window Sealed to Molybdenum Tubing by Metal Soldering	74
4-11	Test Laser Used to Evaluate the Properties of the Space Qualified Laser Design	80

LIST OF ILLUSTRATIONS

<u>Figure</u>	<u>Title</u>	<u>Page</u>
4-12	Test Laser with Coaxial Electrodes	82
4-13	Voltage-Current Characteristics of Coaxial Mock-up Laser Tube	83
4-14	Extrapolation of Discharge Characteristics to Determine Electrode Fall	84

LIST OF TABLES

<u>Table</u>	<u>Title</u>	<u>Page</u>
3-1	Mode Losses for Various Fresnel Numbers for Hemi-confocal Cavity	23
3-2	Summary of Optical Design Parameters of the Space Qualified CO ₂ Laser	24
3-3	Thermal Characteristics of Possible CO ₂ Laser Materials	29
3-4	Frequency Control Parameters	34
3-5	Comparison of Piezoelectric Transducers	37
3-6	Power Supply Specifications Space Qualified CO ₂ Laser	46
4-1	Construction Characteristics of Life Test Lasers Numbers S.Q.-1 and S.Q.-2	61
4-2	Construction Characteristics of Life Test Lasers Numbers S.Q.-3, S.Q.-4, S.Q.-5	62
4-3	Measured Leak Rates for Corresponding Conductance on Beryllium Oxide Samples	78
4-4	Approximate Electrode Fall Voltages for Several CO ₂ Laser Cathode Materials	85

SECTION 1

INTRODUCTION

The development of a space qualified CO₂ laser has been organized into a three phase program covering design (Phase I), development (Phase II) and construction and test (Phase III). This report, which covers the results of the design phase, gives the details of the preliminary laser design as well as the results on experimental studies performed during the first phase.

The object of the first phase of the program is to make a comprehensive examination of all of the factors that bear on the design of a successful space-qualified laser and develop a preliminary design based on the findings. Such factors as resonator configuration, type of discharge, type of cathodes, output mirror transparency, gas mixture and total pressure, laser efficiency, heat removal, frequency stability and amplitude stability, operating and shelf lifetimes, high voltage problems, telemetry requirements, space qualified materials, lift-off and operating environment, etc., have been considered. The second phase of the program will involve breadboarding and design refinement as is necessary, culminating with a design freeze. The third phase will involve construction and complete environmental testing of several deliverable units.

Of the several parameters effecting the operation of the laser, probably the single most important factor is the operating lifetime of the laser tube. Prior to the start of the program, several researchers had announced attainment of greater than 1000 hours of operating life in a sealed-off configuration. All of the studies, however, were performed with comparatively large-sized, high-powered lasers. A considerable portion of this phase of the program has been directed toward life test studies on small CO₂ lasers operating in the 3 watt or less range. On-going tests have to date given operating lifetimes in excess of 3400 hours.

Other experiments which were performed during this phase were 1) improved window sealing techniques, 2) leak rate studies on beryllium oxide (to be used as part of the laser tube vacuum envelope), 3) laser

cold cathode studies, 4) laser efficiency studies on glass mock-up tubes, and 5) optimum mirror transmission studies. The results of these experimental studies are given in section 4. Section 2 is a list of the present laser specifications and section 3 relates the detailed laser design.

SECTION 2

GENERAL SPECIFICATIONS FOR SPACE-QUALIFIED CO₂ LASER

2.1 Laser Head and Electronics Specifications

The following is a list of the general operational specifications of the space-qualified CO₂ laser.

1. To operate at 10.6 μ (P20 transition) with CO₂.
2. To operate in single mode, TEM_{00q}, and single frequency.
3. To be stable in frequency to one part in 10¹⁰ (short-term).
4. To operate at initial power level not less than one watt C.W. Package length shall not exceed twelve inches, two inches of which shall be unoccupied to allow for additional components to be inserted into the resonant cavity.
5. To demonstrate the capability of an operating/shelf life of 3 years, the operating portion of which shall be not less than 10,000 hours. The output power shall not drop below 60% of initial power at 7000 hours and 40% of initial power at 10,000 hours operating time.
6. A completely sealed system with a small reservoir volume is preferred. Other alternatives, such as flowing systems, periodic evacuation and refilling, buffering from high pressure or solid phase reservoirs, or recirculation in flowing systems should be considered only if the sealed system proves to be unattainable. In addition, such alternate scheme shall have sufficient reliability and be self-sufficient so that the required operating life of 10,000 hours will be attained unattended.
7. Sufficient cooling capability shall be provided to maintain full output power with heat sink maintained at 20°C \pm 10°C. All components shall survive (though not necessarily in operation) prolonged exposure to space-craft temperatures up to 150°C.
8. Output shall be polarized, linear to one part in 1000.
9. Beam diameter to be not greater than 1 centimeter.
10. To operate with beam divergence consistent with the diffraction limit for the selected beam diameter. The beam is to be round.
11. To operate within an enclosure with no leakage of stray light.
12. To operate without any significant magnetic (and electric) field leakage.
13. To operate in space vacuum environments after rocket launch.

14. To operate with a minimum angular deviation of the beam axis as a function of temperature, time, vehicle spin, laser age, magnetic field, etc.
15. To operate with a minimum of discharge noise, etc. The final specifications of the over-all power stability will be made consistent with the state-of-the-art at design freeze.
16. To operate with a power supply and control package developed on this contract along with the laser head and meeting identical environmental specifications. Minimum control function could be: (a) turn on supplies, (b) start discharge, and (c) power check telemetry. Any auxiliary equipment (such as for frequency stabilization, cooling, or maintaining the appropriate gas composition in the discharge) should operate with a minimum of external control being required and meet the same environmental specifications.
17. The mounting design shall be as nearly universal as possible, consistent with meeting all other objectives. The design shall permit beam axis alignment with associated apparatus in the satellite assembly phase.
18. The weight, size, and power demand shall be as low as possible consistent with meeting all other objectives.
19. The materials used must be compatible with generally accepted space practice.

2.2 Qualification Test Requirements

The CO₂ Laser Head, power supply/telemetry assembly, and any related components shall initially be qualification tested to withstand the ground, launch, and space mission environments of the Apollo applications launch vehicle and the Apollo command/service module configurations including those using an AAP multiple docking adapter and airlock. It shall perform within specified functional limits during and after exposure (as applicable) to the tests defined below. Tests shall be performed in the sequence listed, except for life tests. Combined environments may be used where feasible and desirable, subject to NASA/ERC approval. MIL-STD-810A "Environmental Test Methods for Aerospace and Ground Equipment" shall be used for methods of tests where applicable, unless otherwise specified below.

2.2.1 Vibration

All components and equipment will be subjected to sinusoidal and random noise vibration in each of three mutually perpendicular axes. Functional tests shall be performed during and after each axis of vibration. Allowable (G-RMS) $\pm 10\%$.

A. Sinusoidal

5-30 cps @0.2 in. double amplitude

30-2000 cps - 8.6G's peak

Traverse frequency range up and back at sweep rate of one octave per minute. Resonance frequencies shall be noted and dwell at main resonance peaks for two minutes.

B. Random

Vibrate for five minutes in each plane

5-30 cps from 0.02 to 0.61 g²/cps

30-700 cps @0.61 g²/cps

700-900 cps @-18db/octave

900-2000 cps @0.18 g²/cps

2.2.2 Shock (Launch)

(Non-operable) The equipment and mounting shall withstand a terminal peak sawtooth shock pulse of 78g peak amplitude for 10 \pm 5

millisecond, including a decay time of not more than 10% of the total duration.

2.2.3 Acoustical Noise

Per the profile outlined below 1/3 octave band acoustical specification $P_c 2 \times 10^{-4}$ Dynes/cm². Test duration - three minutes minimum.

<u>1/3 Octave Band Geom. Mean Freq. (cps)</u>	<u>Db Level</u>
5.0	138.5
6.3	140.0
10.0	142.5
25.0 + 31.5	146.0
40-60	146.0
100	143.0
160	136.0
200	132.5
250	130
500	121
1000	112
1600	105.5
2000	102.5
3150	95.5
4000	92.0
5000	89.0
6300	85.0
8000	81.0
<u>10000</u>	<u>78.0</u>

Overall 156.6 + 4db
- 0db

1/3 octave band sound pressure levels + 4db
- 0db

2.2.4 Acceleration

(Launch) - An acceleration of at least 10g's in each of the 3 axes for at least three minutes (in each axis) - (reentry) - 20g's in each axis for three minutes.

2.2.5 Temperature

(Operational) - Unit shall be cycled over 10°C to 30°C during operation.

2.2.6 Thermal Shock

(Non operational) - Shall be performed per MIL-STD-810A between temperature extremes of -40°C (-40°F) to 74°C (165°F).

2.2.7 Temperature - Altitude

Reduce chamber to 1×10^{-5} torr. Increase temperature to 160°F and then reduce to 0°F in 45 minutes and back to 160°F in another 45 minutes. Perform this cycle (90 minute cycle) six times.

2.2.8 Humidity

10 days of accelerated humidity.

2.2.9 Electromagnetic Compatibility

(EMC) - In accordance with MIL-STD-826.

2.2.10 Operational Life Tests

12 months minimum. Two (2) months to be performed in vacuum (10^{-4} torr or less).

2.2.11 Shelf Life Tests

12 months minimum duration.

2.2.12 Beam Quality

Beam Divergence, Noise and angular stability tests will be conducted and can be included part of functional tests conducted with other environmental tests listed above.

2.2.13 Oxygen Atmosphere

The equipment shall be capable of operating in a pure oxygen atmosphere at 5psi pressure.

2.2.14 Salt Fog Test

Per MIL-STD-810A.

2.2.15 Explosive Atmosphere Test

Per MIL-STD-810A.

SECTION 3

LASER DESIGN

3.1 General and Summary

This section presents the general and detailed design concepts of a 1 watt space qualified CO₂ laser capable of being used for optical communications purposes. During this phase of the program emphasis has been placed on an optimum design for the CO₂ laser head. Some breadboarding of various laser configurations was done to determine many of the design parameters. No breadboarding of the laser high voltage power supply was done, although a preliminary design has been completed.

The major parameters used for the development of the laser design are:

- 1) Size and weight should be as small as possible.
- 2) The efficiency of the laser should be as high as possible.
- 3) The operating voltage should be as low as possible consistent with other objectives.
- 4) The laser should be designed with room for an in-cavity modulator.
- 5) The laser should operate single-wavelength, in a TEM₀₀ mode, with a stable output frequency at the 1 watt level.
- 6) The laser should be conduction cooled.
- 7) The laser must withstand lift-off forces and operate in a space environment.
- 8) The laser tube is to be a sealed system with long life.

To achieve the above goals, a laser design was evolved which has the following major features:

- a) Metal-ceramic laser tube using BeO ceramic for good heat conduction.
- b) Gallium Arsenide Brewster windows on the laser tube.
- c) One cathode - two anode electrode geometry.
- d) gas storage volume of 150 cc.
- e) Invar cavity structure for good temperature and mechanical stability.

- f) Optional electronic stabilization for improved long-term frequency stability.
- g) Dual high voltage power supply with current control.
- h) Weight of laser head and power supply to be approximately 5.9 lbs and 4.2 lbs respectively.
- i) Prime power requirement to be less than 20 watts.

The general concept of the laser is given in Figure 3-1, which shows the laser and associated equipment in block form. The laser is operated by a dual power supply. In the event of failure of one power supply, the laser can operate at reduced power with the remaining unit. During normal operation both units would be in operation. Each power supply is capable of delivering 3.5 kV at 2 mA to the laser tube. The laser and power supplies will use vacuum for the high voltage insulation. To prevent possible breakdown due to insufficient vacuum level, a mechanical pressure interlock is included to preclude turn-on of the power supplies until a preset safe pressure level has been reached.

A portion of the output of the laser is directed to a bolometer detector through an etalon wavelength selector for power monitoring. The proposed etalon is a temperature insensitive resonant structure which is set to transmit the P(20) line at 10.59 microns only. If the laser is not operating on 10.59 microns, then the manual transducer control can be actuated to tune the laser cavity until power is observed on the detector.

Automatic frequency control electronics have been added to the laser as an optional item. Although not necessary for laser operation, it appears to be a desirable feature. The total frequency drift of the laser due to the $\pm 10^{\circ}\text{C}$ variation in the heat sink temperature will be somewhat greater than the oscillating range of a single laser wavelength. Depending on the thermal time constant for the entire system (laser + spacecraft), the laser will periodically jump to another wavelength unless the piezo-electric transducer, on which one of the laser mirrors is mounted, is used to compensate for the thermal drift. In some applications, the AFC

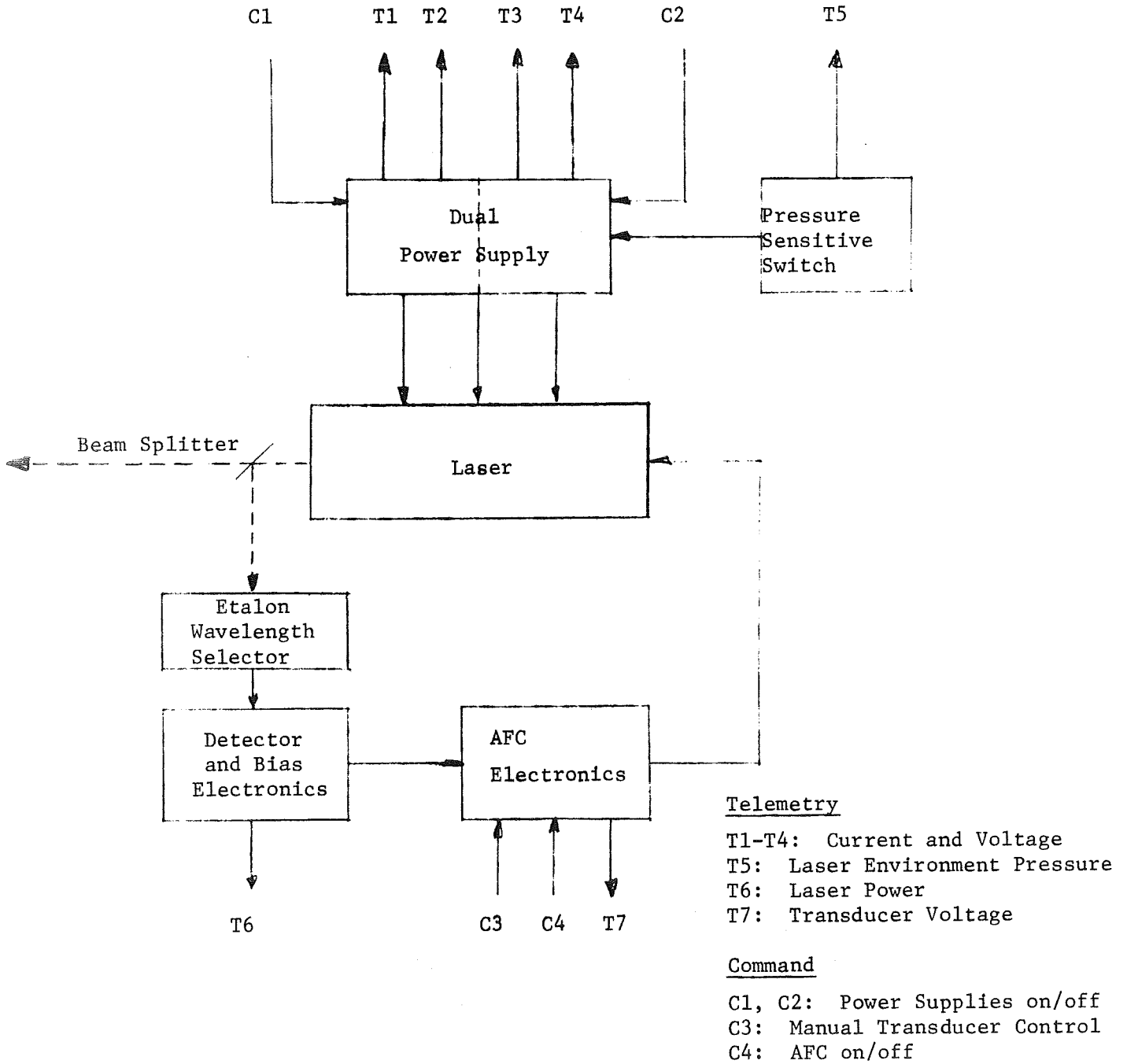


Figure 3-1 Block Diagram, Space Qualified CO₂ Laser Design.

electronics can be operated continuously; on others, it would be used periodically or not at all. The type of laser frequency control to be used would allow tracking of the 10.59 micron line center by the oscillating mirror or "dither" technique described in Section 3.4.3.

The location of the beam splitter, etalon, detector and associated electronics will be external to the laser head. Also, the power supplies will be external. This arrangement facilitates mounting in any proposed optical arrangement and spacecraft configuration.

To achieve the desired specifications for the laser and to make a useful device, many of the laser parameters must be optimized, especially in the area of overall efficiency. However, most of the earlier work on the detailed design of CO₂ lasers has been directed toward attainment of relatively high power; the overall efficiencies quoted for these lasers is not necessarily applicable to very small tubes, where fundamental electrode losses may make up an appreciable portion of the total laser input power. Also, for small lasers, the total gain is rather low, so that losses in the laser optics which may not be significant in higher power lasers play an important role in determining the maximum overall laser efficiency which can be achieved.

Another factor which affects the maximum power output (and, therefore, the laser efficiency) is the thermal environment of the laser. Most laboratory CO₂ lasers are cooled by flowing water around the discharge tube maintaining the laser bore temperature at about 18°C. Since the gain of the CO₂ laser is drastically reduced as its bore temperature increases, the gain of the conduction cooled S.Q. laser will be inherently lower at the maximum spacecraft heat sink temperature of 30°C. To maintain good overall efficiency, it is most important then to design a structure which has a very low thermal impedance between the spacecraft heat sink and the laser bore.

To achieve the operating specifications while attempting to optimize the overall laser efficiency with minimum size and weight, the laser head design as shown in Figure 3-2 has been developed.

Figure 3-2 shows the Brewster Angle laser tube mounted within a rectangular cavity structure. The details of the tube will be discussed in section 3.2. The laser tube (20) is attached directly to the aluminum baseplate (1) of the laser through a large area aluminum heat sink (6). The heat generated in the laser tube is then conducted directly to the laser baseplate, then to the spacecraft heat sink. Each end of the laser is enclosed in a vacuum-tight, bellows-sealed dust enclosure.

Two lightened invar C frames (19) serve as the cavity spacers. The aluminum cavity end frames (12) are mounted to the invar and hold the laser mirrors (15) (23). The mirrors are mounted on a unique ball joint structure (14) (28) which allows mirror adjustment with the aid of a detachable jig (not shown) but can be clamped tightly after adjustment by means of the retainer plate (17), providing a large area contact. The mirror structure is also designed so that the laser mirror assembly can be removed without upsetting the mirror alignment by unscrewing the mirror assembly mounting plate (13).

The opaque mirror is mounted on a piezoelectric transducer (24) of the bimorph variety, which allows relatively large movement in a small size and requires relatively low voltages. This bimorph is capable of enough movement to compensate for the expected thermal drifts of the cavity.

The laser structure is attached directly to the laser base by the use of slip fasteners (9)(10)(11) which allow the invar to move freely with respect to the aluminum base in the direction of the tube axis. The entire unit is housed in a dust cover (21) which may be removed just prior to launch for weight reduction. The laser base is equipped with bolt-down positions along both sides and has two precision machined edges (29) which are accurately aligned with the centerline of the optical beam.

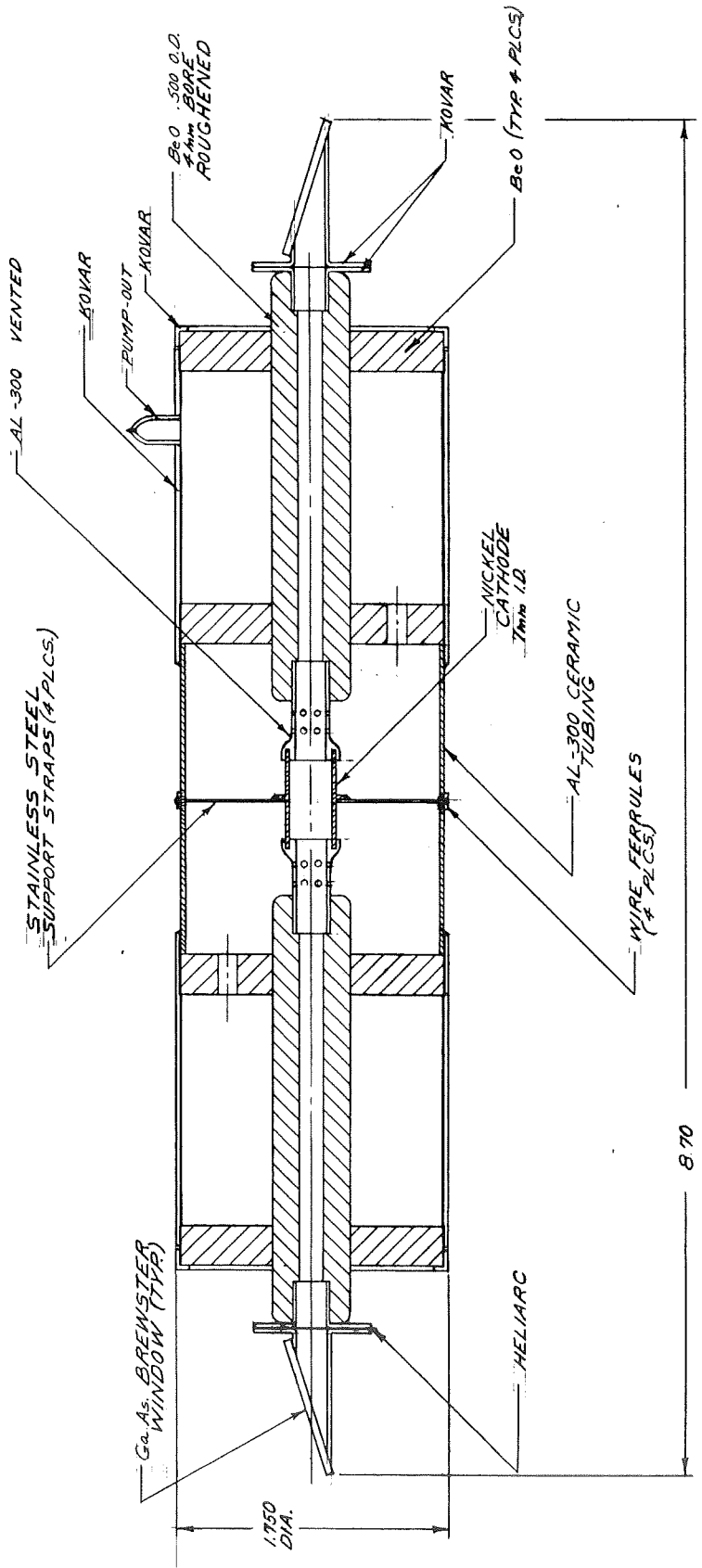
The following sections describe in greater detail the individual elements of this design.

3.2 Tube Design

The laser tube design is based on the following set of major parameters:

- a) The tube must be of sufficient length to provide enough gain for 1 watt minimum output power at the maximum environmental temperature.
- b) The tube must operate with conduction cooling.
- c) The tube must operate with a heated cathode.
- d) The tube must provide TEM₀₀ power only.
- e) The output beam must be polarized.
- f) The tube must have a long operating life.
- g) The tube must be bakeable.
- h) The tube must be rugged to withstand lift-off conditions.
- i) The tube must be capable of operating in a vacuum environment.
- j) The tube should have as high an operating efficiency as possible.

Figure 3-3 is a detailed assembly drawing of the tube design which appears to most closely satisfy the above requirements. To achieve the desired degree of ruggedness, the tube incorporates metal-ceramic type of construction. The tube is of a circular geometry with a 4.0 mm diameter bore made from beryllium oxide. Four 1/4 inch thick BeO fins are located along the tube bore, approximately equally spaced. BeO ceramic was chosen because of its very high coefficient of thermal conductivity and light weight. The outside shell, made from nickel-plated, thin-walled Kovar, serves as a rigidizing structure as well as the vacuum envelope. The spaces between the BeO fins are used as a gas ballast, necessary for increased life, and have a volume of about 150 cc, which is approximately 80 times the active volume. The heat transfer characteristics of this design are quite good: Thermal calculations indicate that the temperature rise from the outside surface of the tube to the hottest spot in the bore (outside the cathode area) will be less than 4°C, even for tube dissipations as high as 15 watts. Therefore, the bore temperature will never exceed about 34°C during operation when the base plate temperature is at its maximum spec. value of 30°C.



SPACE QUALIFIED
LASER TUBE ASSY.

Figure 3-3.

For maximum tube efficiency, the laser utilizes a coaxial electrode structure rather than electrodes in side arms. The Kovar pieces at each end of the laser tube will serve as anodes while the Nickel cylinder in the center of the tube will be the tube cathode. For long life the cathode must be heated to at least 250°C during operation (see section on Laser Life Tests). To achieve this without requiring additional external heat, the cathode has been isolated from the BeO bore by insulating sections of alumina ceramic. To provide the electrical connection to the cathode, as well as additional support, four thin wires of stainless steel run between the cathode and the outside surface of the tube. The wires are terminated on an insulating ceramic tubing so that the cathode may be operated somewhat above ground potential if required. Thermal calculations indicate that this structure will be sufficiently self-heating to allow cathode temperatures somewhat above 250°C to be reached. The major heat loss mechanism from the cathode is by the tube gas to the outside walls.

The advantages of a two anode, single cathode approach over a single cathode, single anode approach are:

- 1) Sputtered material from the cathode is kept farther from the laser windows.
- 2) Total tube voltage is approximately halved.
- 3) Greater power is dissipated at the cathode, since twice the current is being drawn, enabling the cathode to be self heating.

The disadvantages are that the total gain for the same active length is somewhat less, requiring a slightly longer tube, and the higher cathode current may shorten tube life due to a greater sputtering rate from the cathode. Although tests are being performed to determine if the laser lifetime is dependent on cathode current, results thus far are too premature to draw any conclusions. The test laser which is operating at the 3000 + hour level at the writing of this report operates at a cathode current in excess of that expected for the above design, indicating that good lifetime is available at even higher cathode currents than will be

used in the final design. Considering all possibilities, we feel that the three electrode design is the superior approach.

The gallium arsenide Brewster windows will be attached to the end kovar assemblies using hard soldering techniques (see section 4.3), allowing rugged ultra-high-vacuum seals to be obtained. The window assemblies which will be prepared independent of the tube, will then be oriented and heliarc-welded to the tube at the appropriate point in the tube fabrication cycle.

The total length of the tube (8.70 inches) has been chosen to give enough gain to provide 1 watt of output power at the high heat sink temperature of 30°C. At the low heat sink temperature of 10°C, the power output will be approximately 1.2 watts. The gain calculations are carried out in the next section, in conjunction with the optical design.

The diameter of the tube is approximately 1 3/4 inches and the tube will weight about 3/4 lb.

Based on life test data, it appears that the tube will employ a gas mixture of H₂, Xe, N₂, CO₂ and He. The N₂ and He, of course, are used with the CO₂ to obtain high gain and power output. The Xe is added to reduce the starting and operating voltage, and the H₂ to increase tube life by reducing the dissociation rate of CO₂. No automatic pump-out and refill procedures in space are planned for this laser. The tube will be permanently sealed during the processing cycle and will not require further attention. Lifetime tests on similar small lasers have shown promise that the lifetime goals will be met with this approach.

We have observed that, for optimum power output for small bore tubes using mixtures with the above gases, a Pd product for the laser is approximately 3 torr-cm (P is the partial pressure of the CO₂ gas and d is the bore diameter). For the 4 mm diameter ceramic tube, the partial pressure of CO₂ will be quite high, allowing a rather large quantity of CO₂ to be stored in the laser with only a small ballast volume.

3.3 Optical Design

In this section, we consider the optical design of the laser tube and cavity, as well as the gain characteristics of the tube. The optical design presented here is a result of several iterations involving various bore diameters, mirror configurations and total cavity length. We also performed mode calculations for the case of an internal GaAs modulator. Because of the high index of refraction of GaAs, the mode shape changes dramatically when the modulator is added, requiring that the optics be changed to again optimize power output. The laser cavity optics should then be designed to match the specific shape and type of modulator which would be used in the laser.

3.3.1 Gain Characteristics

To optimize the design of a CO₂ laser, it is required that the following parameters be known:

- 1) Gain of the laser as a function of
 - a) gas mixture
 - b) temperature
 - c) bore diameter
- 2) saturation parameter as a function of the same variables.
- 3) expected losses in the laser optics

Once these parameters are known, the optimum design can be obtained by reiterative calculations using various tube geometrics, mirror separations, mirror radii of curvature, etc.

Unfortunately, not all of the above information is yet available for the CO₂ laser, especially in a form which is readily usable. Satisfactorily detailed information on the oscillator saturation parameter for small bore tubes is, in particular, lacking; only estimates based on the operational characteristics of several similar tubes could be used in the calculations.

The power output capabilities of single-mode lasers in terms of mirror transparency, gain and saturation parameter is covered by Garrett⁽¹⁾. Recently, McElroy and Walker⁽²⁾ reformulated the work of Garrett to provide a simple set of parametric curves which are especially applicable to the CO₂ laser.

Figure 3-4 shows these parametric curves, which we have found to accurately describe and predict the characteristics of existing CO₂ lasers. Here the parameter P/K is plotted as a function of the laser single-pass gain and reflectance of the output mirror (non output mirror 100% totally reflecting). The power output, P, can then be calculated once the gain of the laser is known and the parameter K is determined. K is the laser saturation power and is approximately equal to the saturation parameter, W (watts/cm²), times the beam area in the laser bore for the case of uniform spot size in the laser.

Using this approximation for several lasers in our laboratory, we have obtained consistent results when a saturation parameter W of about 250 watts/cm² is used for small bore tubes operating at high pressures.

Also, for the case of small bore tubes (of about 5 mm bore diameter) we have made gain measurements and have found maximum values to be about 5 1/2 dB/meter for sealed systems operating at a 20°C water jacket temperature. No extensive measurements, however, were taken to determine the variation of gain as a function of bore diameter and bore temperature.

The required active laser length can then be calculated once the bore size has been chosen. As will be seen in the next section, a bore diameter of 4 mm seems to be most suitable. Therefore, to obtain the desired 1 watt output,

$$P/K = P/WA = 0.032$$

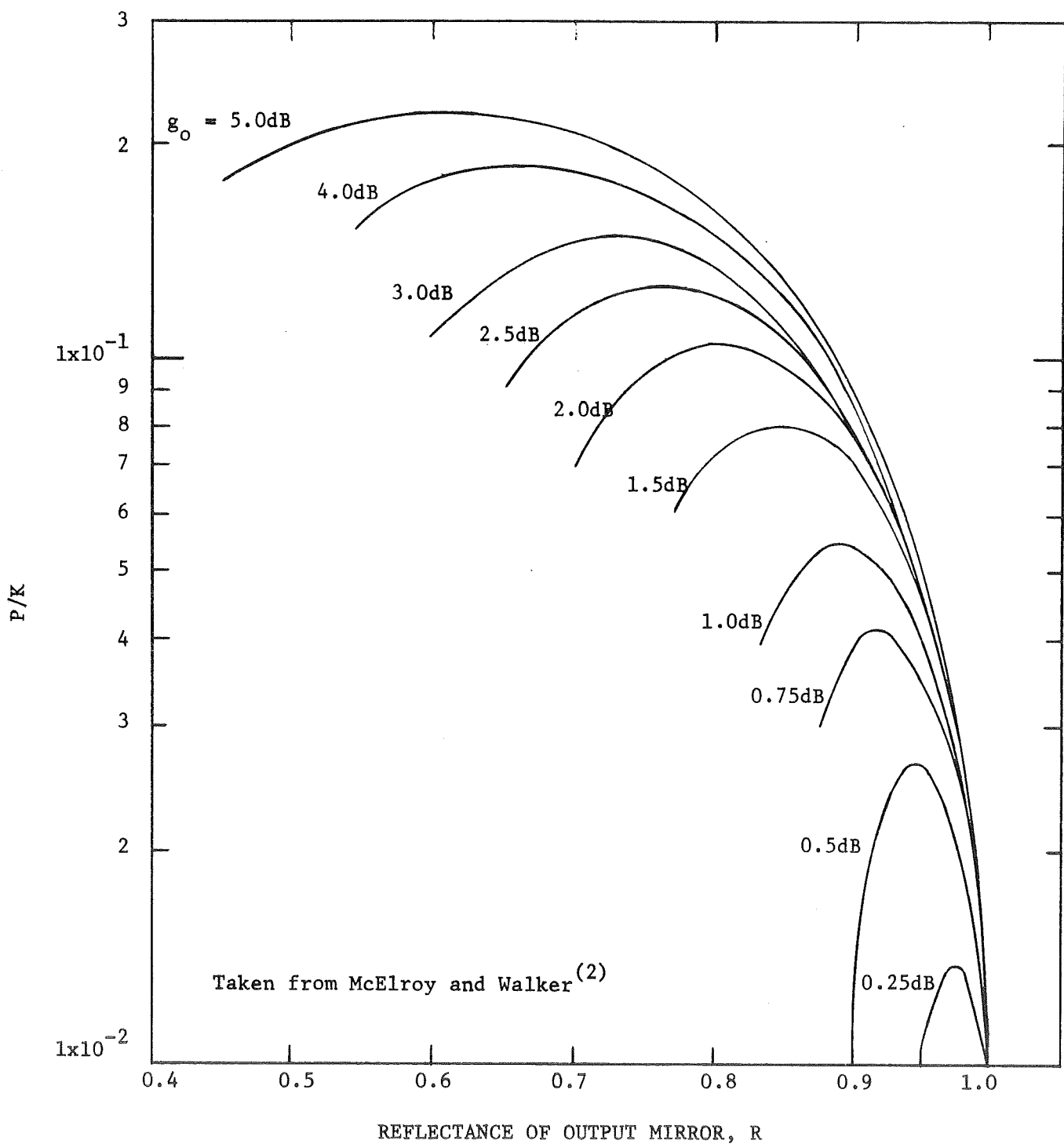


Figure 3-4. Output Power as a function of Mirror Reflectance for a Number of Values for the Single-pass Gain.

From Figure 3-4, the required total gain is about 0.6dB and the optimum mirror reflectivity is about 93%. The active length, l , required to obtain the 0.6dB gain is then

$$l = \frac{0.6\text{dB}}{5.5\text{dB/meter}} = 11 \text{ cm}$$

Since the center cathode region (approximately 3 cm long) will be operating hot and will not contribute significantly to the gain, a total active length of about 14 cm appears to be required.

The above results are calculated for the case of a laser tube operating with a bore temperature of about 20°C. To determine the effects of higher temperature on gain, power output measurements were made on a small-bore quartz laser tube as the temperature of the water jacket was increased. Figure 3-5 shows the results of these measurements.

The maximum temperature of the laser bore during operation is expected to be about 34°C indicating that a power reduction of about 15% below that which would be obtained at 20°C can be expected. To compensate for this power loss, the laser tube has been designed with a 16 cm active length.

Tests on mock-up lasers were performed to verify some of these calculations. The results of these tests are described in Section 4.5.

3.3.2 Laser Bore and Mirror Design

To optimize the power output capability of the laser, the entire mode volume of the laser should be utilized to as great an extent as possible. Operation with mode shapes which have greatly varying sizes from one end of the laser to the other, such as the hemispherical mode, can easily lead to the condition where one end of the tube is operating saturated while the other end is far from saturation. A long-radius mirror configuration provides a fairly uniform optical beam within the laser cavity,

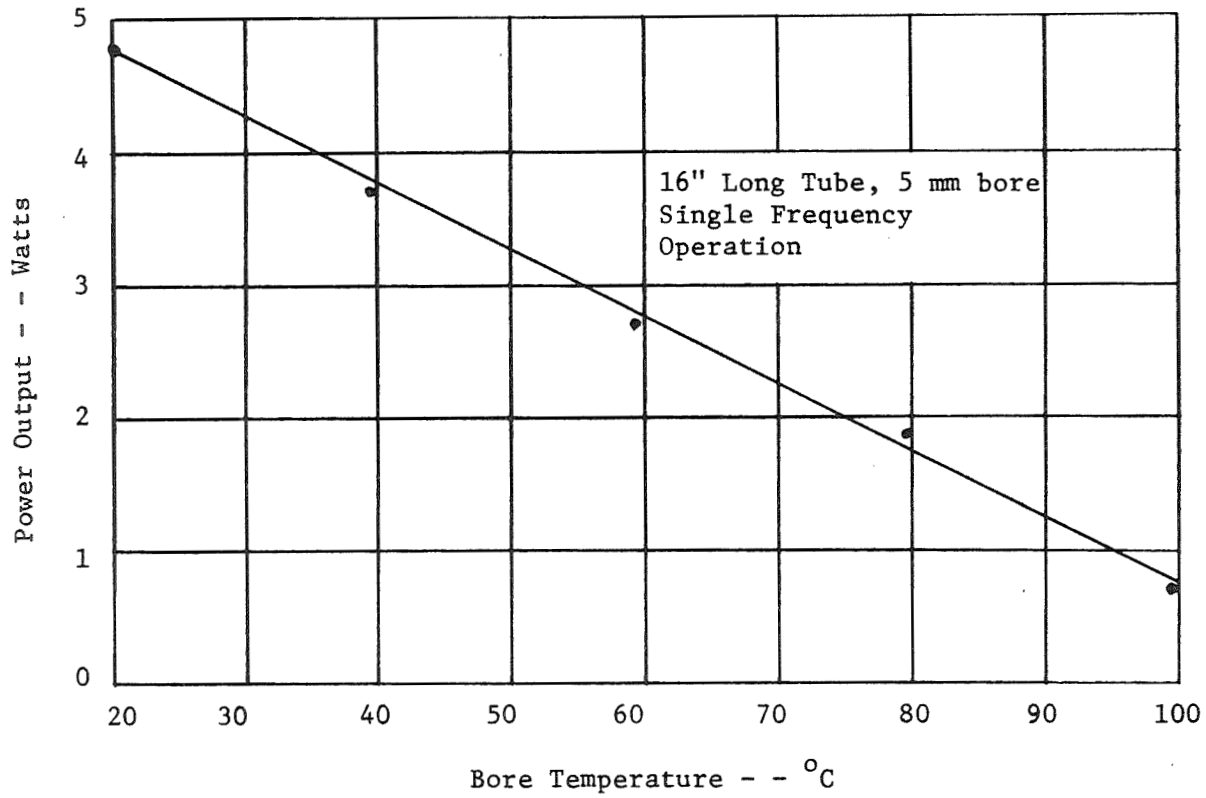


Figure 3-5. Power Output vs. Bore Temperature of Small CO₂ Laser.

but does not offer very good mode discrimination characteristics⁽³⁾. A fairly good compromise design, which provides sufficient beam uniformity as well as excellent mode discrimination between the TEM₀₀ and TEM₀₁ mode is the hemi-confocal cavity.

Assuming that the laser tube is the limiting aperture for the internal optical beam, the Fresnel number, N, for the laser is given as

$$N = \frac{a^2}{L\lambda}$$

where a is the bore radius, L is the optical distance between mirrors and λ is the operating wavelength. Using the computer run diffraction loss curves by Li⁽³⁾ the losses for the TEM₀₀ mode and the TEM₀₁ mode were calculated and are listed in Table 3-1.

<u>N</u>	<u>TEM₀₀ Loss</u>	<u>TEM₀₁ Loss</u>
1.0	5.3%	27%
1.2	2.6%	17%
1.4	1.0%	10%
1.6	0.3%	3.5%

TABLE 3-1

Mode Losses for Various Fresnel Numbers for the Hemi-Confocal Cavity.

To suppress the TEM₀₁ mode from oscillating, the diffraction losses must be greater than the residual gain for this mode. From the curves in Figure 3-4, it can be seen that for the chosen mirror reflectivity of about 93%, the gain for any mode in the laser must be greater than about 0.3dB (8%) in order to oscillate. As seen earlier, the unrestricted gain of the laser tube is about 15% (0.6dB). Therefore, the additional loss required to prevent the TEM₀₁ mode from oscillating is about 7%. From Table 1, a Fresnel number of about 1.4 should provide the required loss to ensure only TEM₀₀ mode oscillation. This Fresnel number is large enough so that the loss to the TEM₀₀ mode is quite small.

The required laser tube bore size can now be calculated once the mirror separation, L, has been established. The mirror separation has been chosen as 28 1/2 cm based on the requirement to allow an open area of 2.0 inches in the cavity for the addition of extra in-cavity components. The bore diameter then is

$$d = 2a = 2 \sqrt{NL\lambda} = 4.0 \text{ mm}$$

The corresponding specifications for the radius of curvature on the mirrors for the hemi-confocal cavity are then

Output Mirror:	Flat
Opaque Mirror:	57 cm

Table 3-2 summarizes the optical characteristics of the laser tube.

TABLE 3-2
Summary of Optical Design Parameters
of the Space Qualified CO₂ Laser

Output Mirror - - - - -	93% Reflecting, flat
Opaque Mirror - - - - -	100% Reflecting, 57 cm radius of curvature
Mirror Separation - - - - -	28 1/2 cm
Type of Cavity - - - - -	Hemi-confocal
Active Length of Laser - - - - -	16 cm
Bore Diameter - - - - -	4.0 mm
Fresnel Number - - - - -	1.4
Power Output Variation with heat Sink Temperature Variation	
from 10°C-30°C - - - - -	1.2 watts - 1.0 watts

3.4 Frequency Stability Considerations

It is the intention that the space qualified CO₂ laser be capable of being used as a communications source. As a result, mode characteristics and frequency stability of the laser are of importance. In almost all of the envisioned applications, the laser will be used in a heterodyne type of system in which a local oscillator laser located at the receiver will be locked in frequency to the transmitter laser. Therefore, long-term frequency drifts in the transmitter will not affect the operation of the system unless the extent of the drift is great enough to push the local oscillator off its operating line. For this reason, a nominal long-term stability figure for the laser can be given as about ± 20 MHz (subject to modification according to the particular application.)

Short-term instabilities, on the other hand, can affect the quality of the communication signal if the rate of frequency fluctuations falls within the information bandwidth of the signal. The tolerable limits on the instabilities again depends on the particular application, but in most cases, stabilities in the kHz range are desired for time periods between 10 to 100 milliseconds.

More than adequate frequency stabilities have been reported in the past⁽⁴⁾ for both the long and short term in rather massive structures. The purpose in the present design is to generate adequate stabilities using the least possible weight and power, but still supply the required mechanical rigidity to withstand the lift-off environment.

Several factors play important roles in the design trade-offs:

- a) Short-term instabilities can be caused by both the environmental acoustical noise and by the ripple from the laser power supply⁽⁵⁾⁽⁶⁾. The amplitude of the acoustical noise in the space environment in which the laser will operate will be substantially below that incurred in a normal laboratory.
- b) The long-term frequency drift is directly dependent on the thermal environment surrounding the laser.

- c) Long-term frequency drifts can be easily tracked out by electronic frequency control techniques⁽⁵⁾.

3.4.1 Short-Term Frequency Stability

To achieve the required mechanical rigidity against vibration, both for the purposes of providing good frequency stability and for successfully withstanding the forces during lift-off, the individual elements of the structure must be designed with geometries and methods of support that do not have low frequency, poorly-damped transverse resonances. In general, the joints between various components of the structure, especially in the area of the mirror mounts, should be designed to have large-area contacts in order to keep the spring constants of the joints high.

These techniques have been used in the design of the present laser in all areas, except possibly in the design of the piezoelectric transducer. The transducer is a unique item and has received special attention. Its design is treated in detail in Section 3.5.

Laser structures similar to that used for this design have been built and tested in our laboratory and have provided short-term stabilities of $1:10^{10}$ in a normal laboratory environment. We feel that substantially better stability figures will most certainly be obtained in the space environment.

The short-term frequency instabilities caused by the laser power supply ripple have been well documented in the literature.⁽⁵⁾⁽⁶⁾ These are caused by variation in the index of refraction of the laser gas with tube current. Typical figures for the frequency shift are on the order of 3/4 MHz/mA for lasers of the size to be used here. To achieve $1:10^{10}$ stability (3 kHz), the ripple current through the tube must be less than about 4 μ A. From the V-I characteristics for tubes of design similar to the space-qualified tube, the change in tube voltage with current is about 110 V/mA at the expected operating current of the tube. The power supply ripple figure must then be less than about 1/2 volt peak to peak. For the

case of a 4000 volt supply, this corresponds to about 0.01% peak-to-peak ripple. The power supply designed for this program has such a ripple figure. It is important to note, however, that this figure applies not only to the ripple content from the converter, which normally operates at a relatively high frequency, but also to the noise content on the space craft prime power supply used to operate the laser.

3.4.2 Long-Term Frequency Stability

The major causes of long-term frequency drifts in the laser are thermal effects which change the physical size or optical thickness of relevant parts of the laser. The operating frequency, f , of a single mode laser is given by

$$f = \frac{c}{2 L_0} q$$

where q is the number of half-wavelengths between the laser mirrors, c is the velocity of light in vacuum and L_0 is the optical distance between mirrors. The change in laser frequency due to a change in cavity length is given by

$$\Delta f = -f \frac{\Delta L_0}{L_0} = -\frac{f}{L_0} \sum_{n=1}^n \Delta L_n$$

where ΔL_n is the optical length change due to each of n various components which contribute to the cavity length changes. Figure 3-6 shows the major elements to be considered here.

The mirrors are separated optically by the Brewster angle windows and the gas discharge, and mechanically by the frame, piezoelectric transducer, mirror substrate and thermal compensator.

Table 3-3 gives thermal properties of the major contributing materials to be used in the CO_2 laser along with their expected physical lengths, ℓ . A few other materials are also listed. As can be seen, the mechanical coefficient of expansion of GaAs is small compared to its

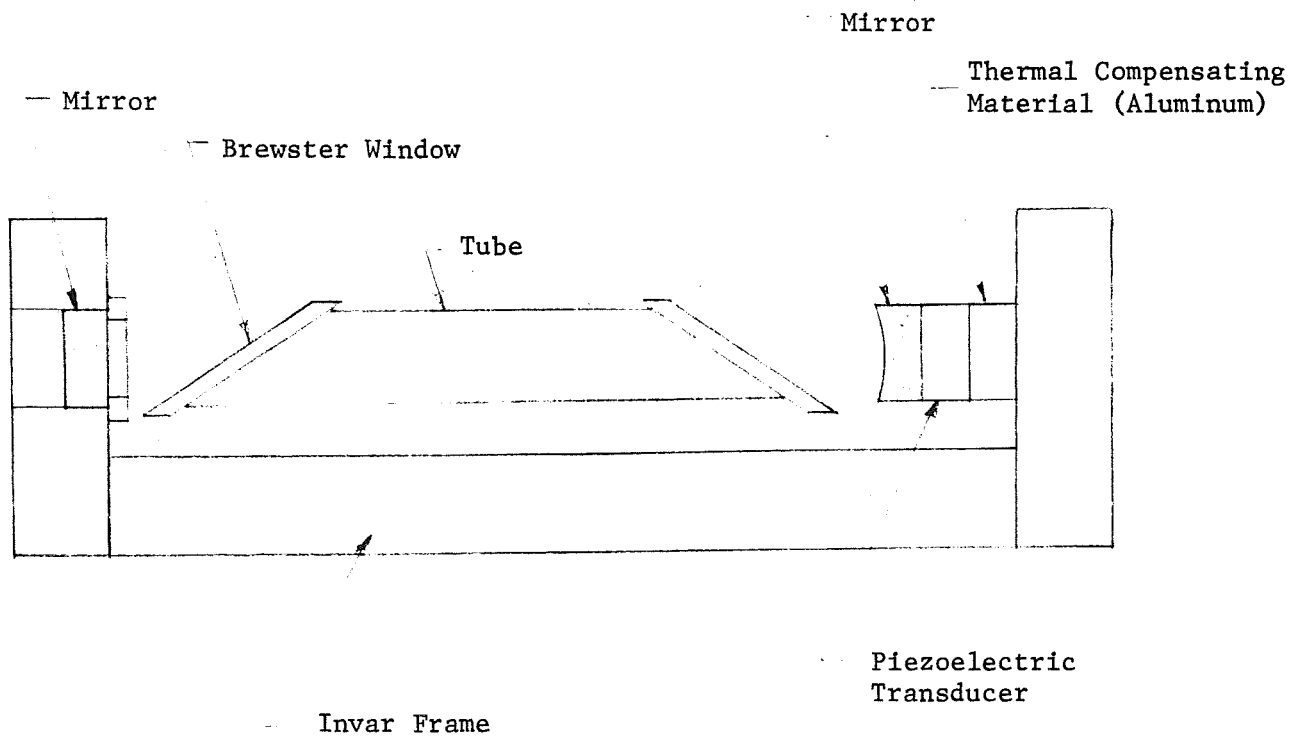


Figure 3-6. Diagram of Laser showing Elements Affecting Frequency Stability due to Temperature Drifts.

optical thickness change with temperature. Using super invar (a special grade of standard invar) and GaAs windows, the thermal sensitivity of the laser can be written as

$$\Delta f = -\frac{f}{L_c} \left[2l_w \left(\frac{dn}{dT} \right)_w + (l\alpha)_I - (l\alpha)_T - (l\alpha)_m - (l\alpha)_{al} \right]$$

and for $L_c \approx 28 \frac{1}{2}$ cm

$$\begin{array}{cccc} \Delta f = -44 \text{ MHz/}^\circ\text{C} & -6.1 \text{ MHz/}^\circ\text{C} & + 0.5 \text{ MHz/}^\circ\text{C} & + 2.4 \text{ MHz/}^\circ\text{C} \\ \text{Windows} & \text{Super Invar} & \text{Transducer} & \text{Mirror} \\ + \frac{f (l\alpha)_{al}}{L_c} & & & \end{array}$$

TABLE 3-3

Thermal Characteristics of Possible CO₂ Laser Materials

<u>Material</u>	$\alpha (^{\circ}\text{C}^{-1})$	$\frac{dn}{dT} (^{\circ}\text{C}^{-1})$	<u>n</u>	<u>Thickness</u>
Aluminum	24×10^{-6}			As required
Invar	1×10^{-6}			
Super Invar	2×10^{-7}			$l_I = 29$ cm
Cervit	1×10^{-7}			
Germanium		$+4.6 \times 10^{-4*}$	4.0	
Windows (gallium arsenide)	6.9×10^{-6}	$+2.1 \times 10^{-4*}$	3.24	$l_w = 0.1$ cm each window
Transducer Ceramic (PZT)	$\sim 5 \times 10^{-6}$			$l_T = 0.15$ cm
Mirror Substrate (glass)	$\sim 5 \times 10^{-6}$			$l_m = 0.3$ cm

* As measured at Sylvania by interference techniques using a stabilized CO₂ laser.

As can be seen, the windows are the major contributors to the long term instabilities of the laser frequency.

If the entire structure can be kept in thermal equilibrium, then

$$\Delta f = -47 \text{ MHz}/^{\circ}\text{C} + \frac{f(\ell\alpha)_{a1}}{L_c}$$

By choosing $\ell_{a1} \approx 1.9 \text{ cm}$, then the effective coefficient of expansion can be made to equal zero.

In practice, it is extremely difficult to obtain a near-zero coefficient of expansion by thermal compensation. Small thermal gradients and variations in α with temperature limit the effectiveness of the compensations. An order of magnitude reduction in the thermal sensitivity, however, is achievable and has been demonstrated in our laboratory. We therefore feel, that a thermal sensitivity figure for the laser of

$$\frac{\Delta f}{\Delta T} \approx 5 \text{ MHz}/^{\circ}\text{C}$$

may be achieved by accurate thermal compensation techniques. This figure would only be applicable after thermal equilibrium in the laser has been achieved. During warm-up, or during some period in which rapid thermal transients were taking place, the laser windows most likely could not be kept in thermal equilibrium with the rest of the laser structure even though they are tied together through the base plate.

Since the Brewster windows are the greatest contributors to the laser frequency instability, selecting a frame material, such as cervit, with an expansion coefficient less than super invar, does not significantly help. Invar has a major advantage that it can be machined to the desired shape (rather than cast) and has very good thermal conductivity compared to other low-expansion materials. Although its density is quite high, the strength of the material is excellent, allowing selective removal of material to reduce its weight.

Since the laser tube must be mounted directly to the base plate to remove the heat generated in the plasma, the window temperature can vary directly with the base plate temperature. For a $\pm 10^{\circ}\text{C}$ base plate temperature environment, the best laser frequency stability will be about ± 50 MHz for the full range of expected operating temperatures. This frequency drift is outside the approximate ± 30 MHz range required for reliable single-wavelength operation; as a result, the laser will periodically change wavelengths when the base plate temperature drifts to the extremes of its range.

To compensate these frequency drifts, an automatic frequency control loop is suggested for use with the laser. It can be arranged that the control loop be actuated only when the frequency goes beyond certain preset limits set by the experimenter, or the control loop can be operated continuously. The following section describes the techniques for obtaining automatic laser frequency control.

3.4.3 Electronic Laser Frequency Control

It is not clear that an electronic control loop for the laser frequency will be required or desired in all the envisioned applications. However, there certainly will be instances when such a control loop will be desirable. As mentioned in the previous section, without some manual or automatic adjustment of one of the laser mirrors through the piezoelectric transducer, the laser will tend to hop to a different wavelength periodically. A simple automatic control scheme, which has been demonstrated in the laboratory⁽⁵⁾, can be used to prevent the large long-term frequency drifts.

Figure 3-7 shows the technique for frequency control, commonly known as the "dither" scheme, since a small oscillation or dither of a laser mirror is required to generate a frequency discriminant. The oscillation of the mirror generates a small FM component on the laser beam. The FM is converted to an AM signal due to the non-linear gain curve of the laser.

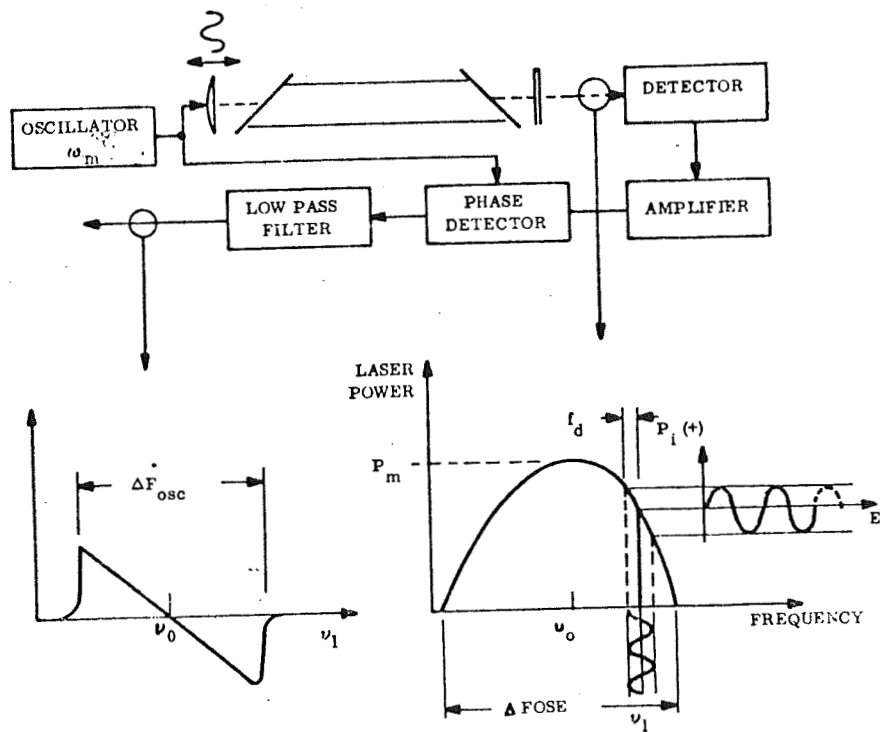


Figure 3-7. Generation and Measurement of the Frequency Calibration Discriminant.

As the laser frequency is swept across the power output curve of the laser at a rate which is slow compared to the dither frequency, the amplitude of the AM signal at the first harmonic frequency of the oscillator which drives the mirror goes to zero at line center.

The equation for the first harmonic voltage signal seen at the detector is given by:

$$v_1(t) = -R \frac{8 P_m f_d}{(\Delta f_{osc})^2} (v_0 - v_1) \sin \omega_m t$$

where:

- R = detector responsivity
- P_m = maximum laser power (at the detector)
- f_d = peak frequency deviation
- v_0 = line center frequency
- v_1 = laser oscillation frequency
- m = modulation frequency

Assuming a minimum detectable voltage signal produced at the input to the first amplifier just equal to the total noise, $V_{n \text{ rms}}$, referred to that point, an expression is obtained for the minimum detectable frequency offset from the line center:

$$(v_0 - v_1)_{\text{min}} = \frac{\sqrt{2} V_{n \text{ rms}} (\Delta f_{osc})^2}{8 R P_m f_d}$$

Values for these parameters which would be applicable to the space qualified laser are shown in Table 3-4. With a modulation frequency of 100 Hz and a peak laser frequency swing of ± 500 kHz, then a long-term frequency stability of about ± 11 kHz should be possible with the best low noise amplifiers.

In laboratory experiments at Sylvania⁽⁷⁾ on 1 watt CO₂ lasers, long term stability figures of ± 20 kHz have been achieved using this

TABLE 3-4

Frequency Control Parameters

<u>Symbol</u>	<u>Description</u>	<u>Value</u>
<u>Laser</u>		
P_m	Maximum laser power on detector	2 mw
f_d	Peak frequency deviation	500 kHz
Δf_{osc}	Effective width of laser oscillation range	200 MHz (1)
ω_m	Modulation frequency (radians)	100 Hz (2π)
<u>Detector and Amplifier</u>		
R	Responsivity at ω_m	2000 mv/mw (2)
$V_n^{(DET)}$ rms	Detector RMS noise voltage in specified bandwidth	2.9 μV (3) (10 Hz)
NF	Amplifier noise figure	1/2 db
V_n rms	Total noise	3.0 μV
<u>System</u>		
$V_1(t)_{min}$	Minimum observable peak AM signal = $2(V_n^{rms} \text{ (total)})$	4.2 μV
$v_0 - v_1$	Laser stability level resulting from system noise (see Equation 2).	± 11 kHz

(1) This parameter is subject to laser gas pressure and mixture conditions and final determination will be made experimentally.

(2) Typical for Barnes germanium-immersed bolometer with 0.25 mm^2 sensitive area and 2.0 millisecond time constant.

(3) Johnson noise typical for 0.5 megohm Ge-immersed bolometer.

technique. It appears that the stability level achievable by the dither approach exceeds the requirements on the laser as far as they are now known.

The actual implementation of the laser frequency control scheme is shown in Figure 3-8. Given a calibration command, the frequency control unit begins slowly tuning the laser frequency while the dither signal is on. The line selection filter, consisting of an air gap etalon 1/2 mm thick (see section 3.6) and a blocking filter, passes energy to the bolometer at only the desired transition. After a signal is received, the bolometer triggers the threshold gate, which stops the initial search control. Simultaneously, the phase detector provides a correction signal that tunes the laser to its own line center. The manual-tune mode disables the lock and allows direct tuning from the ground.

The detail electronics of this control loop have not been designed during this phase but will be considered in the next phase. Present estimates on size, weight and power requirements for the control circuit are 1" x 2" x 4", 0.8 lbs and 1 watt, using thick film techniques.

3.5 Transducer Design

In order to compensate for the long-term thermal drifts and to initially locate the desired wavelength from the laser (P20 transition) an electro-mechanical transducer is required which will allow controlled movement of one of the laser mirrors. The electronic compensation required to track out the thermal drifts was seen in section 3.4.2 to be rather small, on the order of ± 50 MHz, which is equivalent to about $\pm 1/20$ of a wavelength at 10 microns for the proposed cavity size. However, to ensure that the desired wavelength can always be obtained initially, the transducer must be capable of moving $\lambda/2$.

Several types of transducers are capable of providing this movement, 1) stack-of-plates transducer, 2) cylindrical transducer, and 3) bender-bimorph transducer. Table 3.5 compares these transducers for

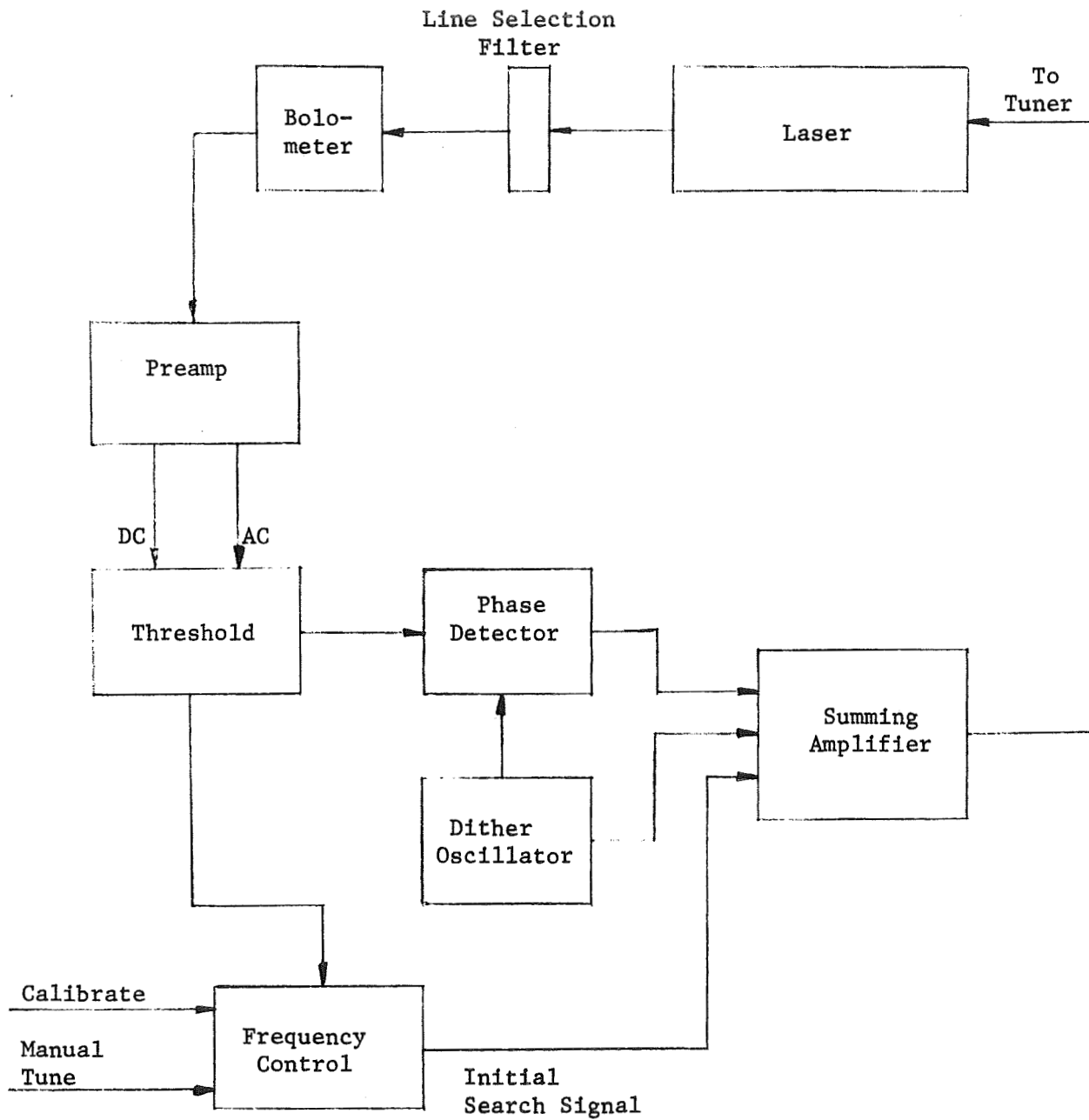


Figure 3-8. Laser Frequency Control

TABLE 3-5

Comparison of Piezoelectric Transducers

<u>Item</u>	<u>Stack of Plates</u>	<u>Cylindrical</u>	<u>Bimorph</u>
Typical Transducer Length Re- quired to obtain 5 μ movement (cm)	1.5	3.5	0.15
Required voltage to obtain 5 μ movement (volts)	400	1000	110
Unloaded resonant frequency (kcps)	100	42	3.6

configurations which would be appropriate for the space qualified CO₂ laser. The comparison gives only approximate values to indicate the various trade-offs involved. The bimorph transducer requires much less physical space and requires substantially lower operating voltage over the other units. Although its resonant frequency is low, it is not substantially below that expected for the overall laser structure.

The stack-of-plates transducer utilizes several epoxied plates connected electrically in parallel but mechanically in series to provide relatively large motion but with only the voltage required for one plate. The plates operate on a thickness expansion mode. The cylindrical transducer is a single unit with electrodes on its inside and outside surfaces. It is poled so that as voltage is applied, the length of the cylinder changes. This mode of operation is not as efficient as that for the stack-of-plates transducer, requiring much higher voltages and a larger size.

A "bimorph" or "bender" transducer is a piezoelectric device made from two thin, plate-shaped transducer elements bonded together in such a manner that when one contracts in length, the other expands. This provides a bending motion when one end of the transducer is allowed to remain unconstrained. If the bender is clamped at both ends, with a mirror mounted in the center of the bender, as shown in Figure 3-9, then the mirror can be translated without tilting.

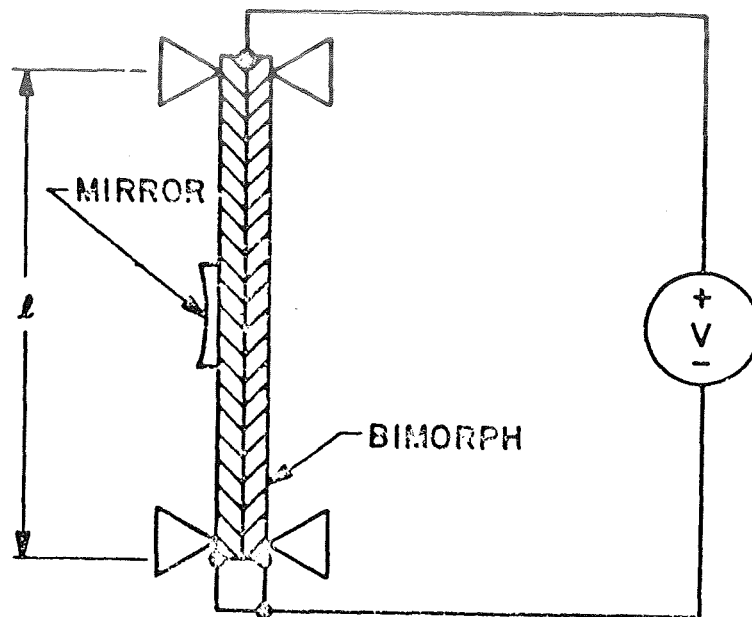


Figure 3-9. Doubly Clamped Bimorph With Laser Mirror Mounted.

The pertinent approximate equations which describe the operation of the bimorph are given by *

$$x = d_{31} V \frac{l^2}{t^2} \quad) \text{ Linear bimorph, edge clamped}$$

$$f_r = 60 \frac{t}{l^2} \quad (\text{kHz})$$

where x is the mirror displacement in meters, d_{31} is the piezoelectric coefficient in meters/volts (166×10^{-12} for Glenite G-1500 material), V is applied voltage, l is the length in inches, t is the total bimorph thickness in inches, and f_r is the fundamental resonant frequency of the bimorph. Also of importance in the design of bimorph transducers is the voltage limits which must be observed. The thin bimorphs proposed have an electric field limit of about 10 volts/mil.

Tradeoff analysis involving size limitation in the laser package, maximum voltages, mounting configurations and environmental stress levels

* Handbooks from Gulton Industries and Clevite

indicates that a linear bimorph with the following characteristics will be most suitable:

Length:	1.0 inch
Width:	0.25 inch
Thickness:	0.060 inch
Maximum safe voltage:	600V
Normal voltage range:	0-110V
Normal displacement:	0-5 microns
Resonant frequency:	3.6 kcps

The low voltage operation of the bimorph puts it below the minimum of the Paschen breakdown curve⁽⁸⁾ for all values of pressure and gas composition, thus removing the potential problem of arcing in the space environment.

In order to maintain as high a resonant frequency as possible for the transducer assembly, the mass of the laser mirror must be kept to as low a value as possible. It appears feasible to attach a small substrate to the transducer prior to the final polishing and coating of the mirror. The substrate would then be polished to a thickness of about 1/2 mm and then coated. Using this approach will allow the weight of the mirror to be less than 5% of the weight of the transducer, resulting in a drop of the resonant frequency by only about 200 cps. Since the resonant frequency will remain above 2000 cps, the lowest resonance will be above the vibration test environment, and the transducer should have no problem passing qualification tests.

3.6 Power Monitor and Wavelength Identifier

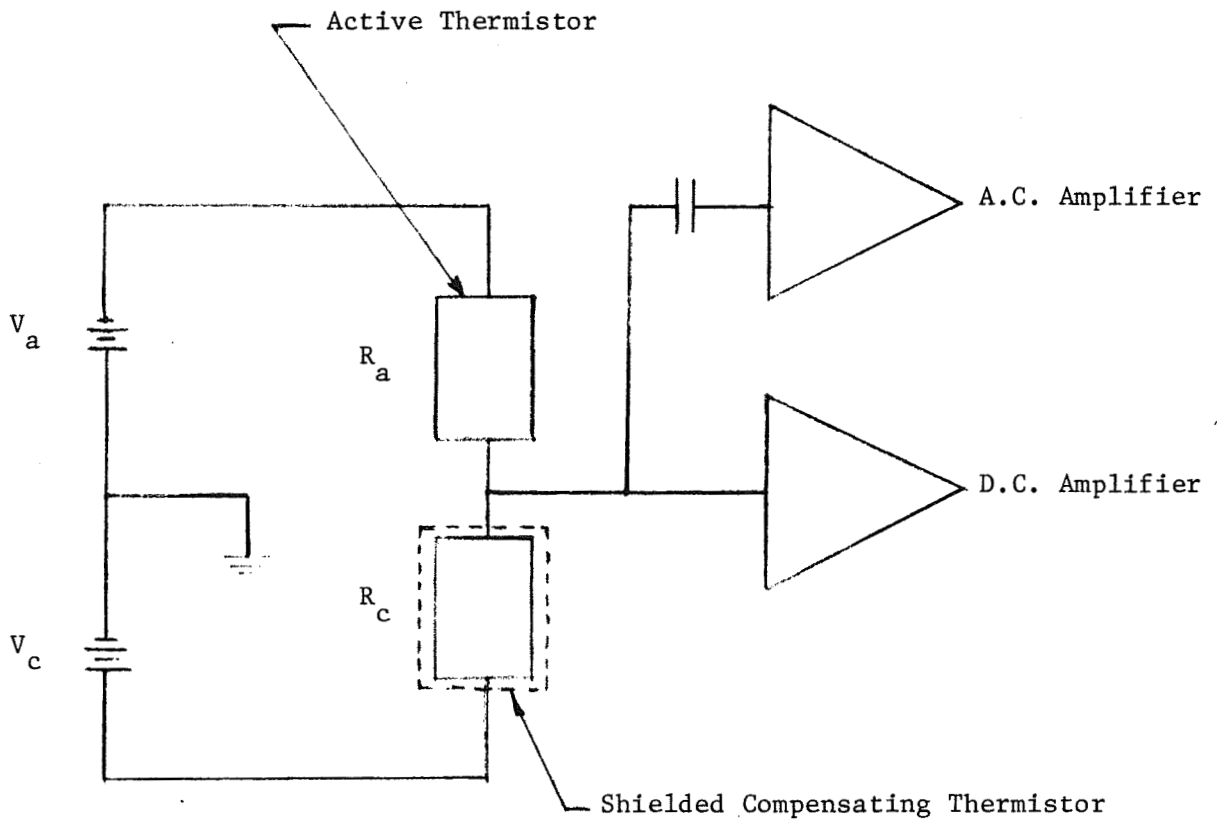
3.6.1 Power Monitor

A thin film thermistor bolometer has been chosen as the power monitor detector for the laser. The device uses two thermally sensitive thin film resistor flakes which undergo a large change in resistance when exposed to radiation. In normal use these are connected by a simple bolometer bridge arrangement shown in Figure 3.10. Equal bias voltages of opposite polarity are applied to the two flakes, keeping their common junction close to ground potential. Because the characteristics of the two units are accurately matched, they tend to exhibit equal resistance changes when ambient temperature changes occur. When radiation is concentrated on the active flake, its resistance changes and the unbalance in the circuit is amplified. For power output measurements a D.C. amplifier is required. For the electronic frequency control loop an A.C. amplifier can be added.

3.6.2 Wavelength Identifier

The CO₂ laser is capable of operating on a number of different wavelengths near 10.6, 10.2, 9.6, and 9.3 microns. By choosing the proper coating characteristics of the output mirror, the laser can be forced to oscillate in the 10.6 micron band without difficulty; however, several wavelengths are still available in this band and can oscillate. In moving one of the laser mirrors in an axial direction, a number of different lines can be obtained as the laser cavity resonance first coincides with the gain curve of one P(J) transition, then another. To ensure that the P(20) transition is oscillating, some wavelength discrimination technique must be employed.

Unfortunately, the use of permanent in-cavity wavelength selection devices such as prisms and gratings will drastically reduce the power output capability of the laser. The technique which has been chosen for this program uses an air or vacuum gap etalon plate, which is tuned to transmit only the P(20) line, in front of the power detector. This technique does not restrict the laser to operating only on the P(20) transition, but it does allow automatic or manual setting of the laser to the proper wavelength.



$$V_a = V_c, \quad R_a = R_c$$

Figure 3.10 Bolometer Electrical Circuit.

The etalon is a resonant structure which has pass bands every $c/2L$ in frequency space. Here c is the velocity of light and L is the separation of the mirrors. By making the length or thickness of the etalon sufficiently small, the resonant characteristics can be adjusted to allow only one of the possible lines which would normally operate in the 10.6 micron band to pass through the etalon with significant power.

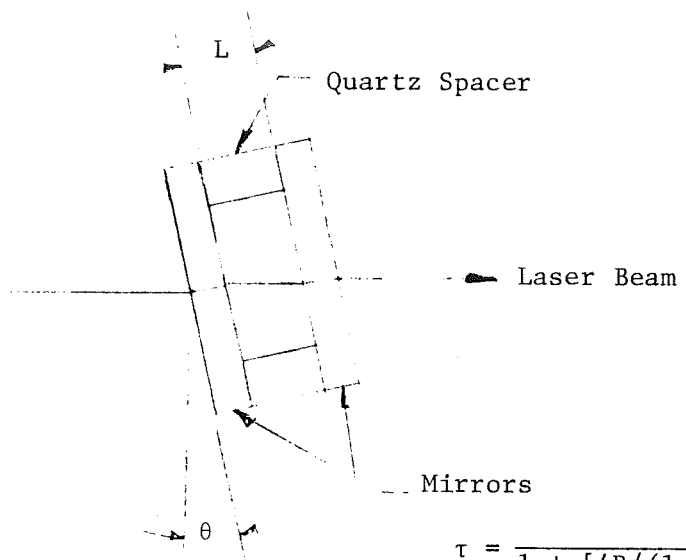
Figure 3.11 schematically shows the etalon along with the transmission characteristics. The transmission of a lossless plane parallel etalon of length L , and equal mirror reflectivities R is given by (14)

$$\tau = \frac{1}{1 + [4R/(1-R)^2] \sin^2(2\pi)(L \cos \theta/\lambda_0)},$$

where λ_0 is the free space wavelength of the incident radiation and θ is the angle of tilt of the etalon. The resolution, or finesse, F , which is the ratio of the frequency separation between successive transmission peaks, $c/2L$, to the transmission bandwidth is given by

$$F = \frac{\pi R^{1/2}}{1-R} = \frac{c/2L}{\Delta\nu}$$

An ideally manufactured device (no loss due to absorption or scattering in mirror coatings and no reflectivity mismatch between mirrors) would have a periodic pass band characteristic as shown in Figure 3.11. The transmission peaks would be 100 percent, and the transmission nulls would be near zero for fairly large R . As described by the above equations, the position of the transmission peaks in absolute frequency space is determined by the angle which the plate makes with the beam and the actual thickness of the plate. The wavelength for maximum transmission ($\tau = 1$) occurs when $2\pi L \cos \theta/\lambda_0 = m$, or $\lambda_0 = 2L \cos \theta/m$, where m is an integer representing the number of half wavelengths between mirrors.



$$\tau = \frac{1}{1 + [4R/(1-R)^2] \sin^2(2\pi L \cos \theta / \lambda_0)}$$

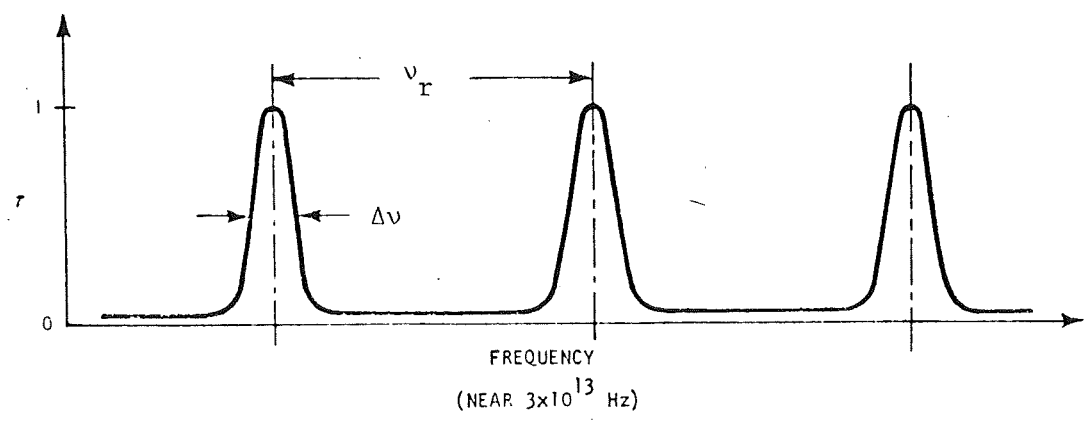


Figure 3.11 Pass Band Characteristics of a Short Fabry-Perot Etalon.

Choosing an etalon thickness of about 1/2 mm, the resonant transmission peaks will be separated by

$$\nu_r = 300 \text{ GHz}$$

Since the P(J) lines are separated by about 50 GHz, the etalon will discriminate against ± 5 lines around P(20). That is, the etalon will not pass (with significant amplitude) P(10) through P(18) or P(22) through P(30) when set in angle to pass P(20).

The angular sensitivity of the etalon certainly is tolerable. Near normal incidence, $4\text{-}1/2^\circ$ represents a change in m by one. The etalon will have to be located and fixed in angular position to within about $1/4^\circ$, which is well within normal optical tolerances.

To ensure good pass band characteristics, a finesse of greater than about 20 should be obtained. This will ensure that no other wavelengths will have significant transmission when the etalon is tuned to the P(20) transition. The corresponding mirror reflectivities are then about 86 percent.

The device is quite insensitive to temperature fluctuations if a suitably low coefficient of expansion material is used for the spacer. For example, if quartz is used ($\alpha = 1 \times 10^{-6}/^\circ\text{C}$), then the device can fluctuate over $\pm 100^\circ\text{C}$ before a significant detuning effect will occur.

The etalon technique for wavelength selection and identification has been used many times in the past at Sylvania⁽⁵⁾. Most of the previous work, however, has used solid etalons rather than air gap etalons. The operation of these devices is the same as described above, except that most of the highly transmitting materials for use at 10.6 microns have large values of dn/dT (such as Gallium Arsenide at $2 \times 10^{-4}/^\circ\text{C}$) and as a result are quite temperature sensitive. The air gap etalon will not require any temperature stabilization other than that provided by the spacecraft temperature control.

3.7 Power Supply Design

3.7.1 General

Experiments with our life test lasers have indicated that as the laser approaches the end of its useful life, the current for maximum power output slowly drops. At certain stages, the power output can be roughly doubled by reducing the laser current. These results have indicated the desirability of designing the laser power supply with variable current capability. The design of the power supply should be capable of providing the following functions:

- a) automatic starting of the laser tube
- b) redundant dual configuration
- c) current regulation
- d) current level set
- e) telemetry outputs for current and voltage.

Table 3.6 is a list of the power supply specifications required to drive the laser. The power supply described in the rest of this section uses variable frequency control and variable pulse width with flyback voltage conversion to obtain regulated output voltage and high efficiency over a wide range of output power. The pulse width is varied to maintain output power constant over a wide range of input voltages.

The input-to-output power-conversion efficiency of a conventional converter is typically 70 to 80 percent at full output power, but drops off at less than full output power due to fixed losses in the drive and control circuits. The power supply described here uses less than one percent of its output power in the unloaded condition. The overall efficiency is greater than 80 percent over a wide range of output power.

Table 3.6

POWER SUPPLY SPECIFICATIONS
SPACE QUALIFIED CO₂ LASER

- 1) Input Voltage 28 VDC \pm 4 Volts
- 2) Output Voltage (at Ballast Resistor) 3500 VDC
- 3) Output Current 3.0 mA
(each supply)
- 4) Current Regulation \pm 5%
Over full input voltage swing and load
impedance variation of \pm 20%
- 5) Current Adjust. Step adjustment from
1.5 mA to 3.0 mA in
0.5 mA steps
- 6) Ripple Less than .01% rms
- 7) Telemetry Output (voltage and current) 0-5 VDC
- 8) Starting Circuit Overvoltage capability
to be provided until
laser draws current.

3.7.2 Circuit Description

Figure 3.12 shows a block diagram of the power supply, and Figure 3.13 shows a simplified circuit for the control circuitry of the power supply. A sample of the output voltage (or current) is applied to the reference amplifier input. This sample is compared to a constant reference voltage from a Zener diode. The difference output from the reference amplifier is used to control the frequency of the voltage controlled oscillator. For example, if the output voltage from the reference amplifier is high, the frequency of the oscillator is lowered. The output of the oscillator is used to trigger a one shot multivibrator which provides a constant output pulse width and voltage level. Variations in the input voltage are used to vary the pulse width of the one shot. With a constant output voltage, an increase in the supply voltage causes a decrease in pulse width. Therefore, under constant load conditions, the energy in the output pulse is constant.

The output pulse is used to drive the input to the voltage converter, Figure 3.14. The sharply rising V_{be} pulse saturates Q_1 , bringing the collector voltage to nearly ground potential as shown in Figure 3.14c. While the collector is near ground, the unregulated input voltage appears across the primary of the output transformer.

At the end of the V_{be} pulse, Q_1 begins to turn off, causing the polarity of the transformer primary to reverse. This flyback effect increases the collector voltage to a value greater than the input supply voltage as shown in Figure 3.14c. The energy stored in the field of the transformer is transferred to the output capacitor, C_o because a decreasing current in the primary induces a voltage in the secondary in the correct direction for current to flow through the diode. This flyback technique, that is opening an inductive circuit to obtain an energy transfer, provides a lossless energy transfer if all components are ideal, and low-loss transfer even with non-ideal components. This same technique has been used at Sylvania in switching regulators with very good efficiency.

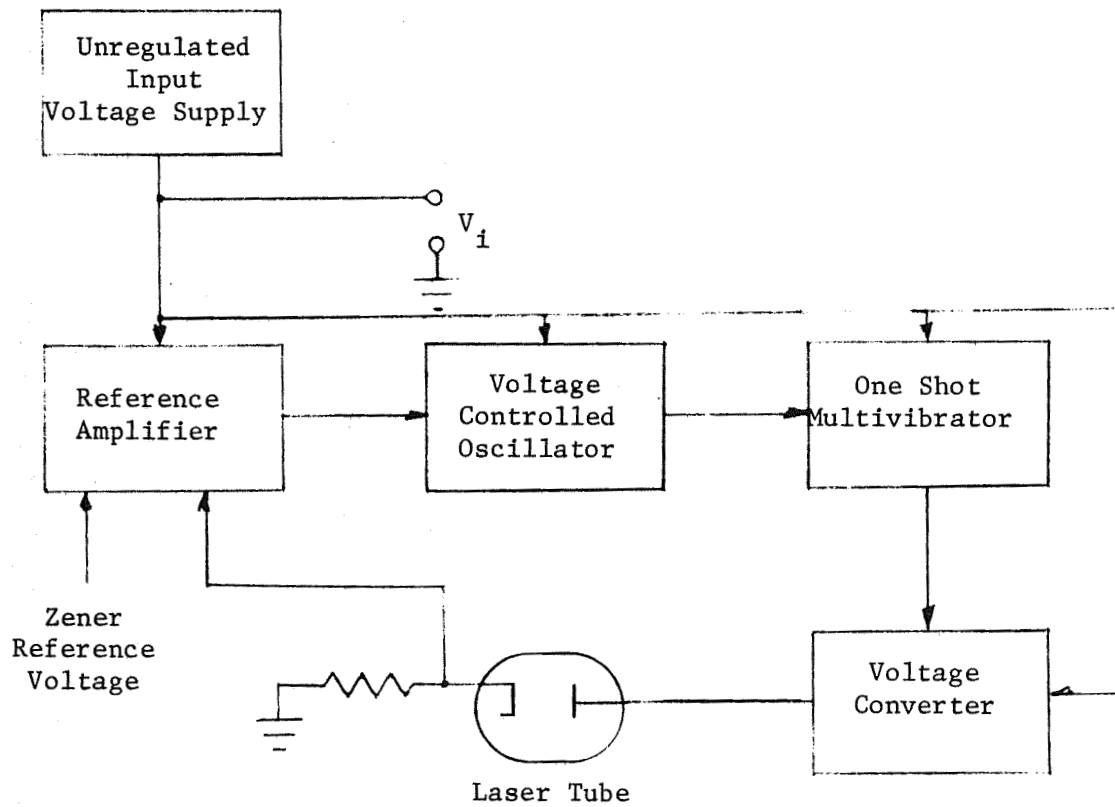


Figure 3.12 Power Supply System Block Diagram.

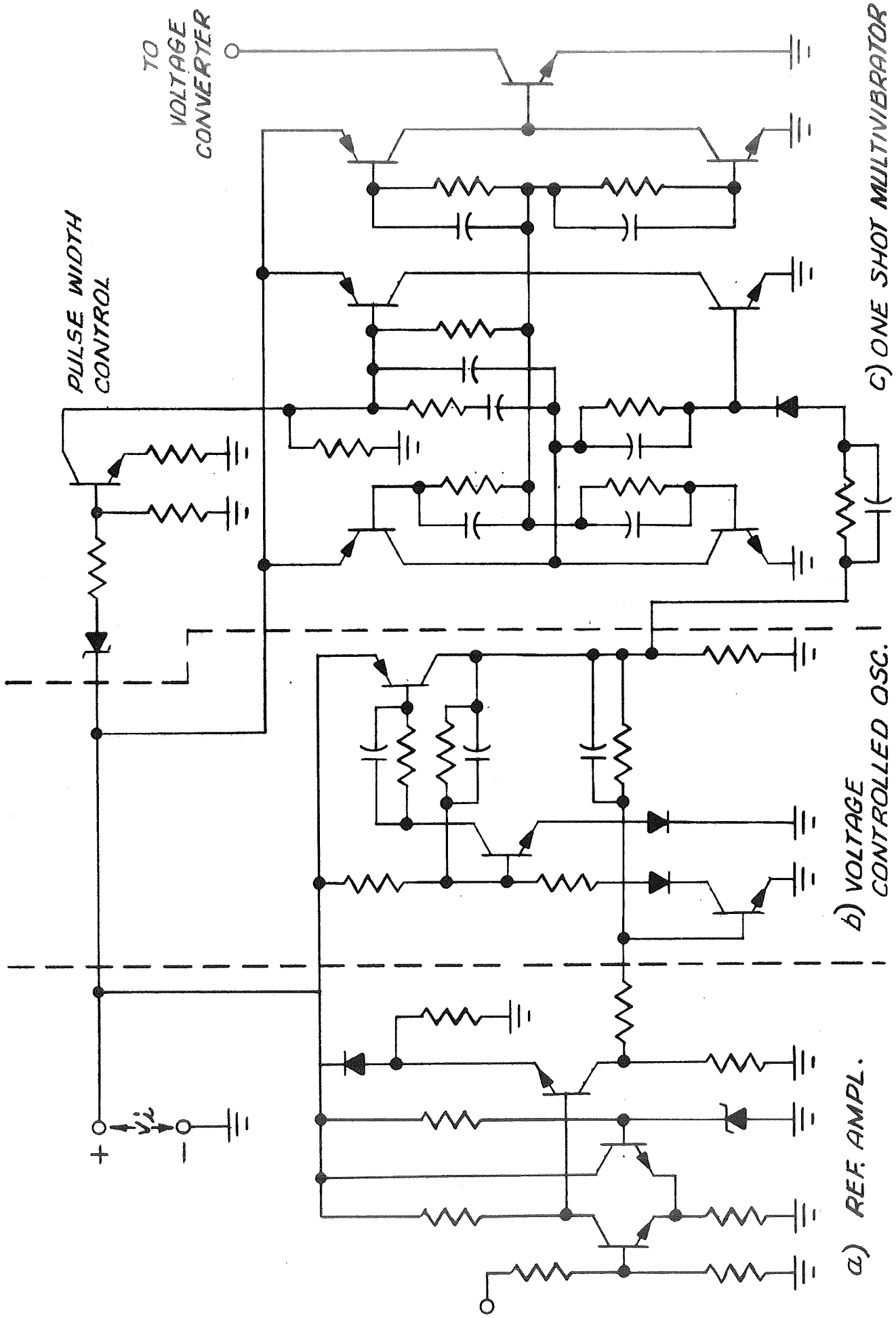
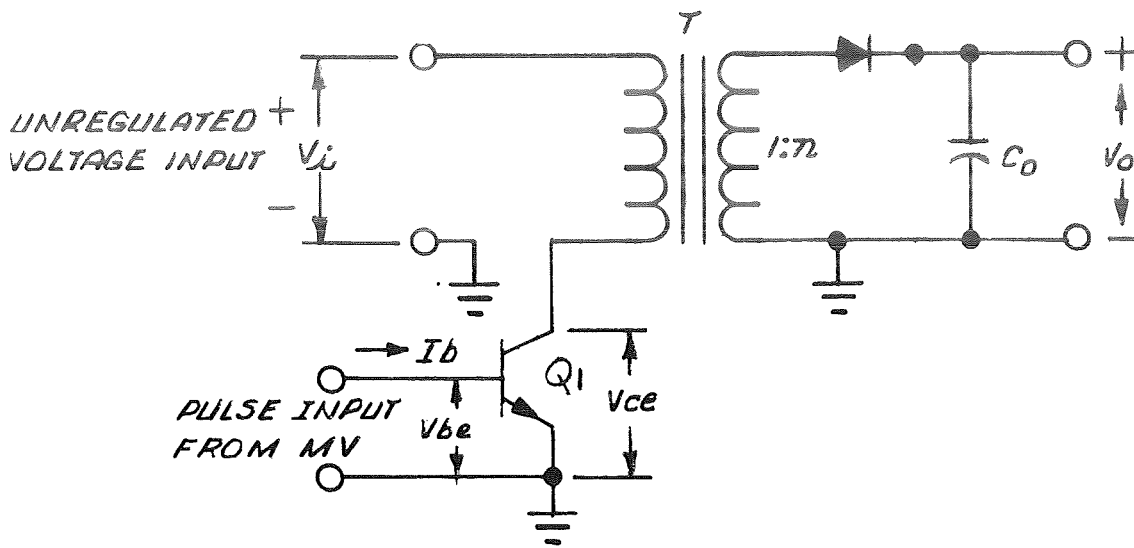
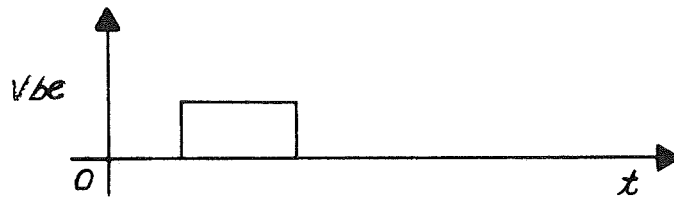


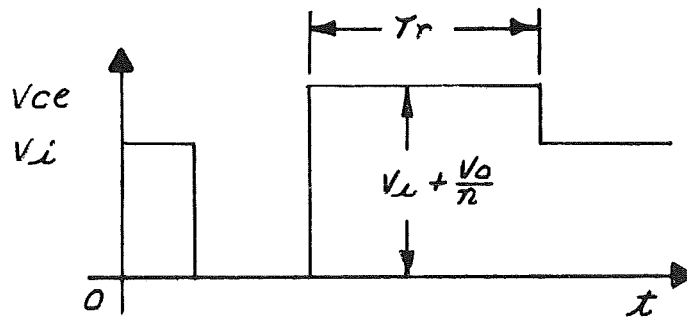
Figure 3.13 Typical Simplified Circuit.



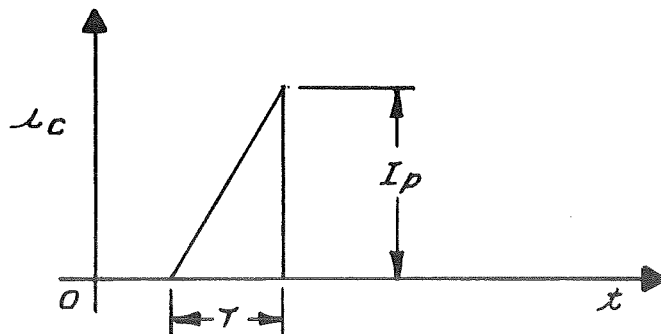
a) CIRCUIT



b) MV OUTPUT PULSE



c) COLLECTOR VOLTAGE



d) COLLECTOR CURRENT

Figure 3.14 Voltage Converter and Waveforms.

3.7.3 Starting Circuit

Whenever power is applied, the power supply will supply 5 kV pulses until the laser fires. When the laser fires, the supply will regulate at the programmed current level at approximately 3.5 kV

3.7.4 Command Circuit

Four current levels may be programmed externally. Magnetic latching relays and diode "OR" gates provide a memory for the last command. A +28 volt pulse, 10 milliseconds long, is required to set the relays for the proper command. The diode "OR" gate will only accept one command at a time. In the event that two commands are given at the same time, the relays will oscillate for the duration of the command with the final resting state indeterminate.

3.7.5 Monitor Outputs

Two monitor outputs are provided, an output voltage and output current monitor with the following characteristics:

Output Level = 0 V to +5 V D.C.

Output Impedance = 10K Minimum

3.7.6 Packaging

Extensive use of thick film techniques will allow most of the discrete components to be replaced by a 1" x 2" thick film circuit. The power transformer, power transistor, relays and filter capacitors will be mounted to the chassis. For each of the dual supplies, the following specifications apply:

Estimated Size = 2" x 2" x 9", 36 in³

Estimated Weight = 2.1 lbs.

Estimated Efficiency = 80 percent;

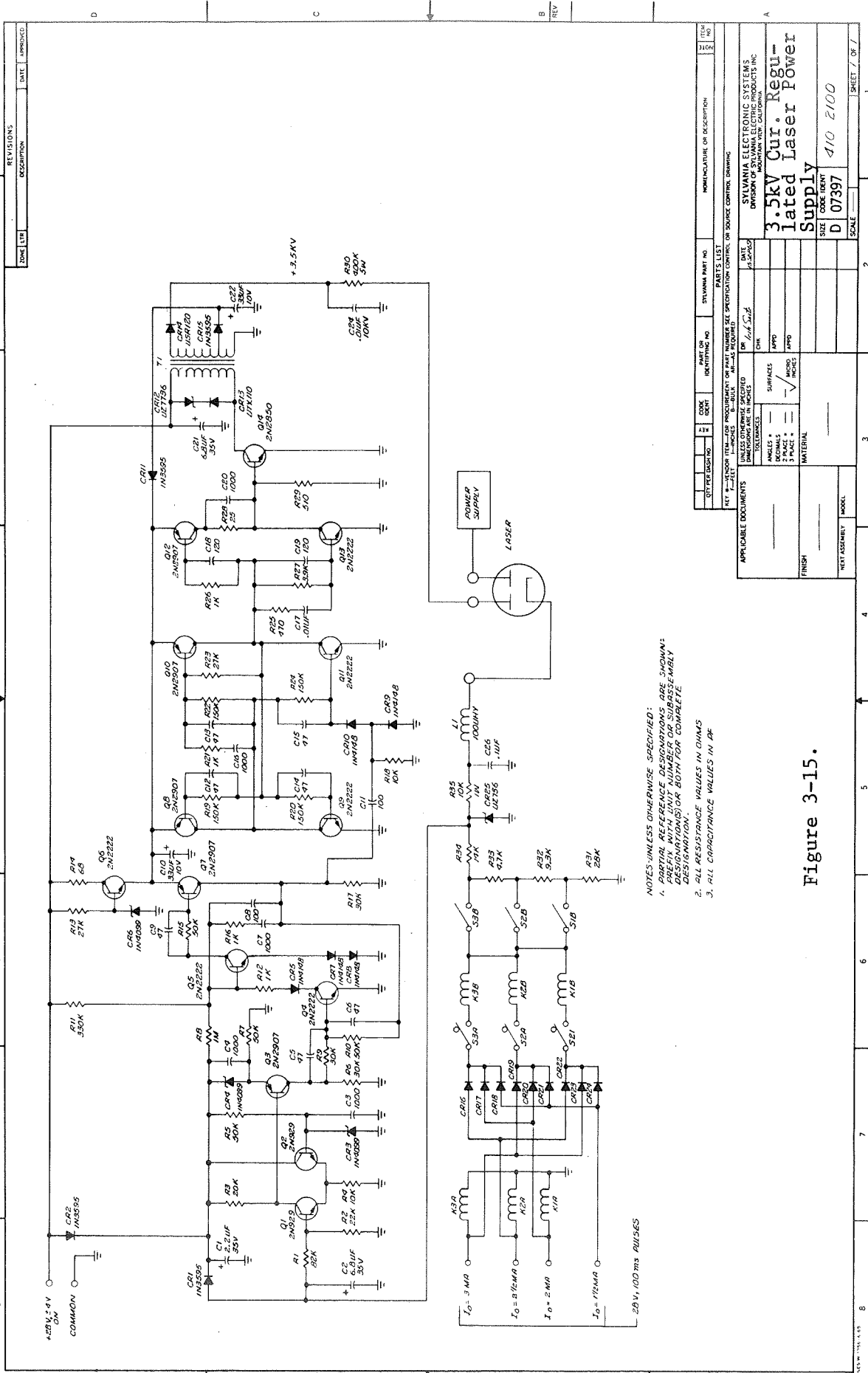
Voltage Output = 3kV to 5kV D.C.

Current Output = 1.5 mA to 3.0 mA

Ripple \leq .01 percent rms.

The overall package will be RFI tight, with filtering on all leads entering or leaving the package. Two such packages are required for the laser tube, making the total estimated power supply weight 4.2 lbs.

Figure 3.15 is a detailed schematic of the proposed power supply. This supply will be breadboarded and tested during the next phase.



- NOTES: UNLESS OTHERWISE SPECIFIED:
1. PARTIAL REFERENCE DESIGNATIONS ARE SHOWN: PREFIX WITH UNIT NUMBER OR SUBASSEMBLY DESIGNATION(S) OR BOTH FOR COMPLETE.
 2. ALL RESISTANCE VALUES IN OHMS.
 3. ALL CAPACITANCE VALUES IN μF .

Figure 3-15.

REVISIONS		DATE		APPROVED	
NO.	DESCRIPTION	DATE	BY	DATE	BY
1					

KEY 1 - BLOCK LETTER OR PROTOTYPE OF PART NUMBER OR SPECIFICATION SYMBOL OR SOURCE CONTROL DRAWING	KEY 2 - BLOCK LETTER OR PROTOTYPE OF PART NUMBER OR SPECIFICATION SYMBOL OR SOURCE CONTROL DRAWING
UNLESS OTHERWISE SPECIFIED DIMENSIONS ARE IN INCHES	UNLESS OTHERWISE SPECIFIED DIMENSIONS ARE IN INCHES
1 SURFACE	1 SURFACE
2 SURFACES	2 SURFACES
3 PAGES	3 PAGES
4 PAGES	4 PAGES
5 PAGES	5 PAGES
6 PAGES	6 PAGES
7 PAGES	7 PAGES
8 PAGES	8 PAGES
9 PAGES	9 PAGES
10 PAGES	10 PAGES
11 PAGES	11 PAGES
12 PAGES	12 PAGES
13 PAGES	13 PAGES
14 PAGES	14 PAGES
15 PAGES	15 PAGES
16 PAGES	16 PAGES
17 PAGES	17 PAGES
18 PAGES	18 PAGES
19 PAGES	19 PAGES
20 PAGES	20 PAGES
21 PAGES	21 PAGES
22 PAGES	22 PAGES
23 PAGES	23 PAGES
24 PAGES	24 PAGES
25 PAGES	25 PAGES
26 PAGES	26 PAGES
27 PAGES	27 PAGES
28 PAGES	28 PAGES
29 PAGES	29 PAGES
30 PAGES	30 PAGES
31 PAGES	31 PAGES
32 PAGES	32 PAGES
33 PAGES	33 PAGES
34 PAGES	34 PAGES
35 PAGES	35 PAGES
36 PAGES	36 PAGES
37 PAGES	37 PAGES
38 PAGES	38 PAGES
39 PAGES	39 PAGES
40 PAGES	40 PAGES
41 PAGES	41 PAGES
42 PAGES	42 PAGES
43 PAGES	43 PAGES
44 PAGES	44 PAGES
45 PAGES	45 PAGES
46 PAGES	46 PAGES
47 PAGES	47 PAGES
48 PAGES	48 PAGES
49 PAGES	49 PAGES
50 PAGES	50 PAGES
51 PAGES	51 PAGES
52 PAGES	52 PAGES
53 PAGES	53 PAGES
54 PAGES	54 PAGES
55 PAGES	55 PAGES
56 PAGES	56 PAGES
57 PAGES	57 PAGES
58 PAGES	58 PAGES
59 PAGES	59 PAGES
60 PAGES	60 PAGES
61 PAGES	61 PAGES
62 PAGES	62 PAGES
63 PAGES	63 PAGES
64 PAGES	64 PAGES
65 PAGES	65 PAGES
66 PAGES	66 PAGES
67 PAGES	67 PAGES
68 PAGES	68 PAGES
69 PAGES	69 PAGES
70 PAGES	70 PAGES
71 PAGES	71 PAGES
72 PAGES	72 PAGES
73 PAGES	73 PAGES
74 PAGES	74 PAGES
75 PAGES	75 PAGES
76 PAGES	76 PAGES
77 PAGES	77 PAGES
78 PAGES	78 PAGES
79 PAGES	79 PAGES
80 PAGES	80 PAGES
81 PAGES	81 PAGES
82 PAGES	82 PAGES
83 PAGES	83 PAGES
84 PAGES	84 PAGES
85 PAGES	85 PAGES
86 PAGES	86 PAGES
87 PAGES	87 PAGES
88 PAGES	88 PAGES
89 PAGES	89 PAGES
90 PAGES	90 PAGES
91 PAGES	91 PAGES
92 PAGES	92 PAGES
93 PAGES	93 PAGES
94 PAGES	94 PAGES
95 PAGES	95 PAGES
96 PAGES	96 PAGES
97 PAGES	97 PAGES
98 PAGES	98 PAGES
99 PAGES	99 PAGES
100 PAGES	100 PAGES

4.0 EXPERIMENTAL STUDIES

4.1 Introduction

During the course of the program several experimental studies were performed in order to develop a better understanding of the operational characteristics of low power CO₂ lasers and to develop techniques for extending tube lifetime and increasing tube reliability.

Our studies included:

- a) life test experiments on CO₂ lasers
- b) development of metal-soldering techniques for the attachment of GaAs Brewster windows
- c) study of porosity characteristics of beryllium oxide
- d) efficiency and power output tests on mock-up laser tubes
- e) determination of fundamental electrode losses for several cathode materials.

The following sections describe the results of these studies.

4.2 Laser Life Tests

4.2.1 General

During this phase of the program, life tests on several low power CO₂ lasers were performed. A life test station with mass spectrometer gas analysis capability was constructed and an ultra-high vacuum technique for monitoring the total gas pressure of each laser tube was devised. The longest-lived tube, which is presently operating at the 3400 hour mark, uses a heated nickel cathode of the type first described by Carbone⁽⁹⁾.

4.2.2 Life Test Station

A block diagram of the life test station is shown in Figure 4-1, with a photograph of the station in Figure 4-2. An EAI QUAD 150 residual gas analyzer with its associated oil free pumping system, shown in Figure 4-3, is attached to a glass manifold whose volume is accurately calibrated.

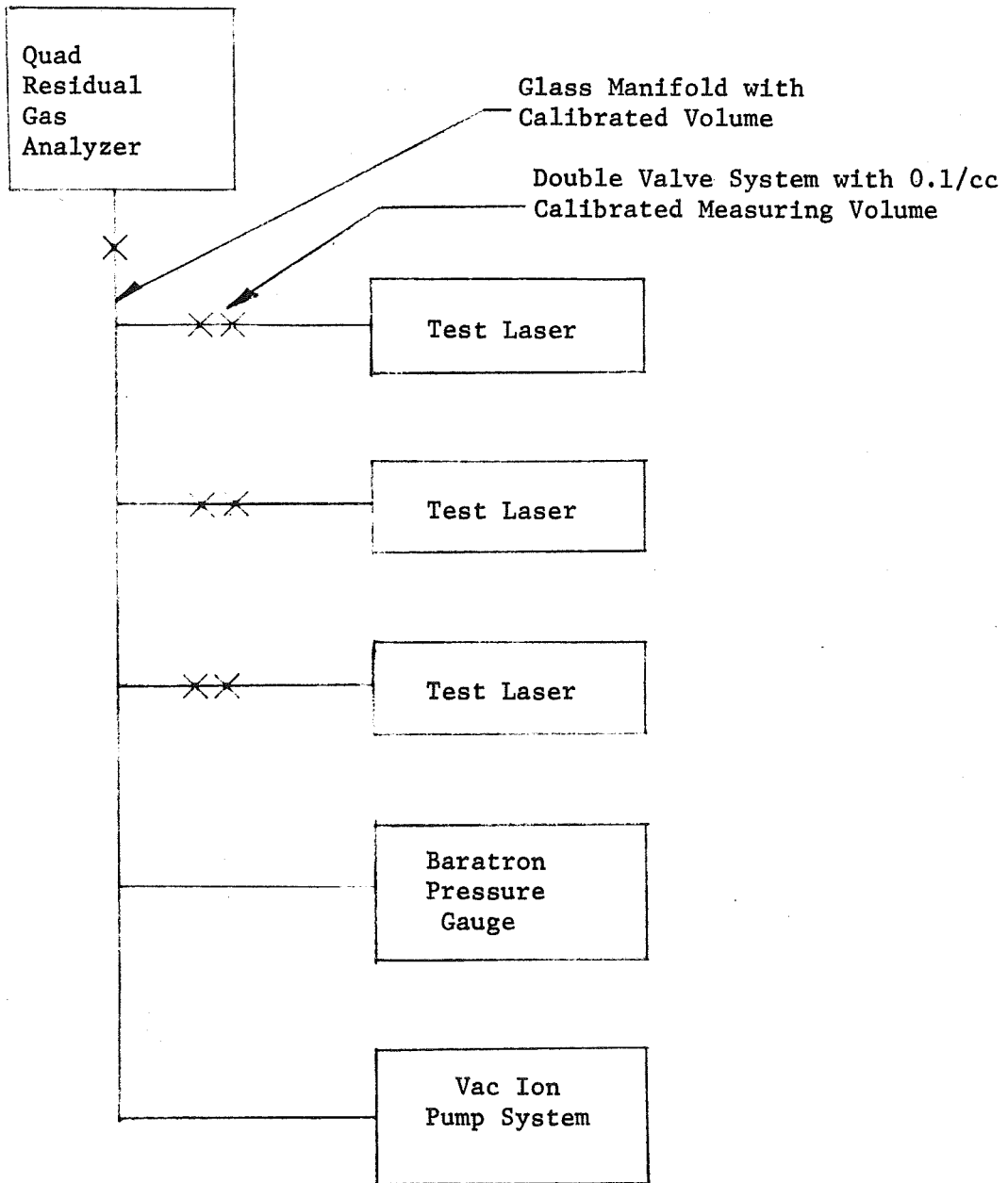


Figure 4-1. Laser Life Test Station Block Diagram.



Figure 4-2. Photograph of Life Test Facility.

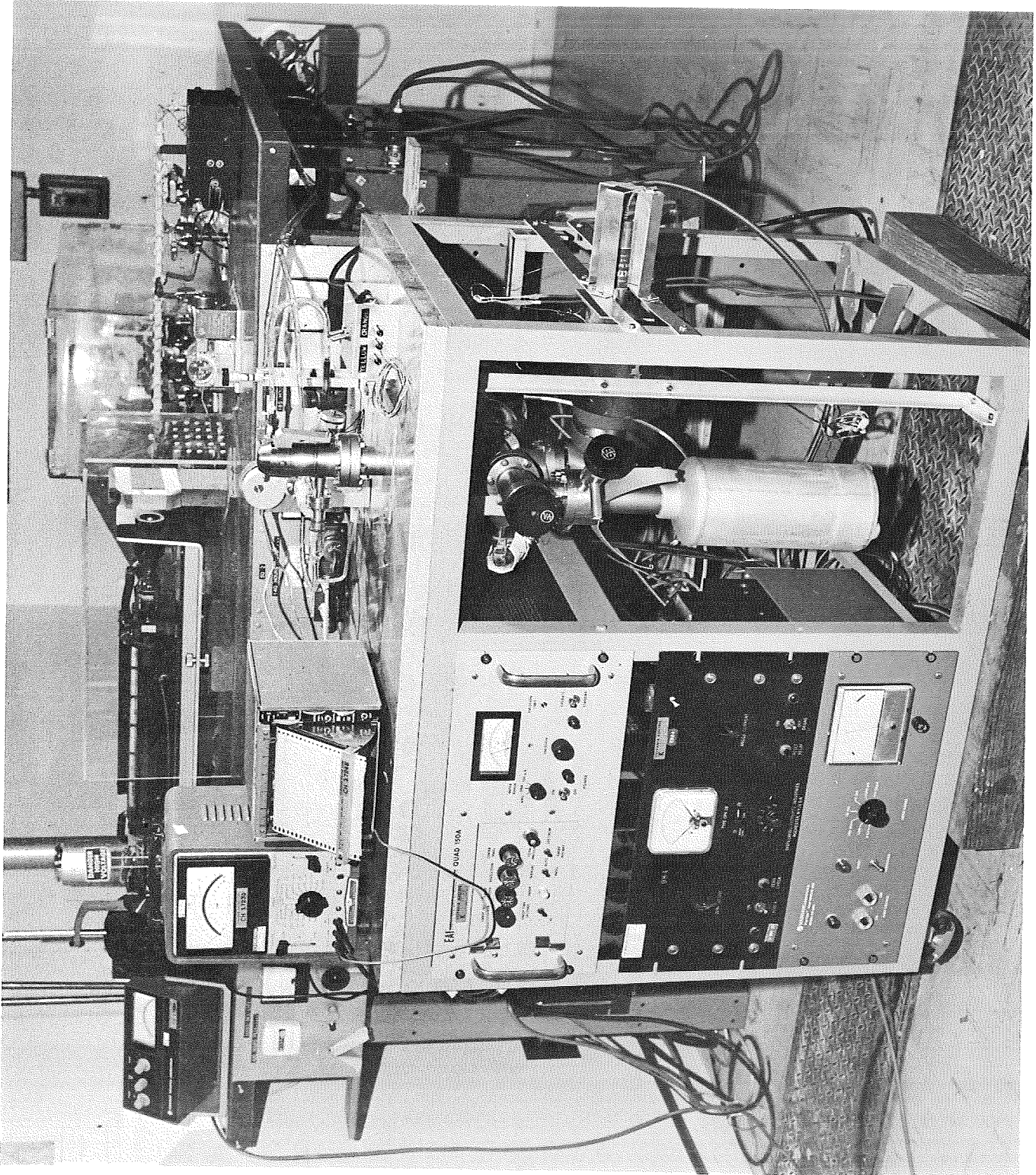


Figure 4-3. Residual Gas Analyzer.

The pressure in the manifold (independent of gas mixture) can be measured accurately with an MKS Baratron capacitive manometer pressure gauge. In normal operation, a life test laser is connected to the glass manifold through a special sampling valve made by Varian Associates. This all metal, bellows sealed valve allows withdrawing approximately 0.1 cc of gas from the laser tube. The sampling volume of each valve is accurately calibrated so that the pressure measured by the Baratron gauge is directly proportional to the pressure in the laser tube. The residual gas analyzer then provides data on the partial pressures of the gases in the laser tube.

Unfortunately, due to the long delivery time on many of the special components for this system and the relatively lengthy calibration procedures, the system was not entirely operational until after several of the life test lasers had compiled a significant number of operating hours. Therefore, gas analysis data on the tubes during their early operating stages are incomplete. Data on later tubes and on future tubes, however, will be more complete.

The special sampling valve shown in Figure 4-4 is actually two valves constructed in such a manner that the valve seats are separated by a very small volume. A solenoid-actuated driver is used to open and close the appropriate valve stem. The valves are constructed from stainless steel, have a bellows-sealed stem and use gold O-rings on the valve seat. Sampling volumes from near zero to several cubic centimeters are possible by properly designing the center section of the valve. For our system, 0.1 cc sampling volume provides enough gas to raise the pressure in the manifold to the 10 micron range, well into the high accuracy region for the Baratron gauge. The amount of gas removed by the 0.1 cc sampling volume is quite small compared to the approximately 300 cc of stored gas in each laser tube, allowing a large number of samples to be taken before a significant drop in tube pressure is noticed.

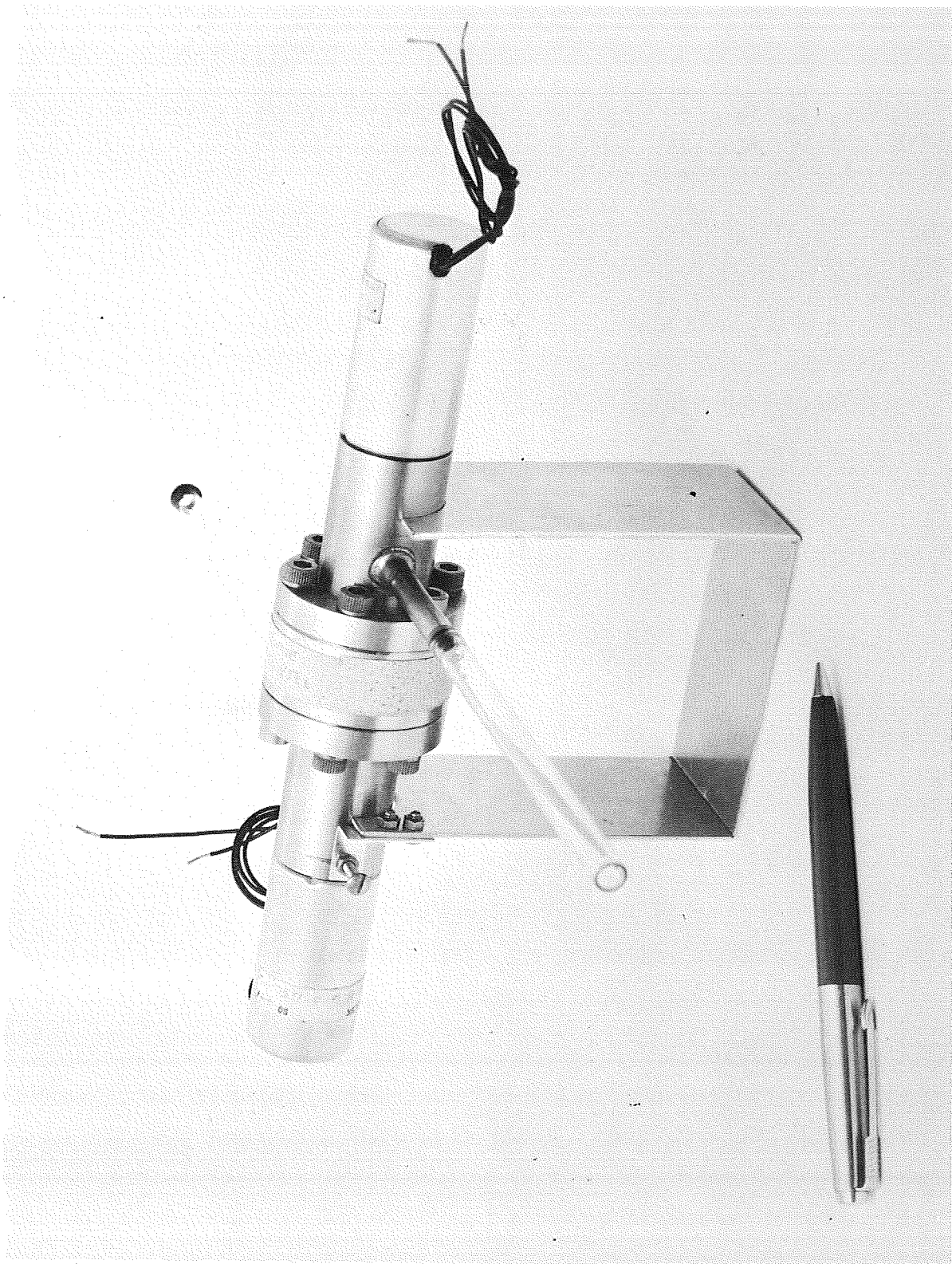


Figure 4-4. Calibrated Gas Sampling Valve.

4.2.3 Description of Life Test Lasers

During the course of the program, the requirements on the size and power of the space qualified laser were changed from a 5 watt power output unit to a 1 watt unit. As a result, the design of the life test lasers changed slightly to better simulate the characteristics of the lasers to be used in the final design. Tables 4-1 and 4-2 list the important features of these lasers. In all cases, internal mirrors were used and were attached to the laser tube structure by "Torr-seal" epoxy (trademark of Varian Associates).

The germanium etalon output coupler used with S.Q.-1 and 2 provided a mirror transmission of about 22%, which was slightly higher than optimum. As a result, a reduction in gain of the laser shows up as a larger change in power output than would be seen if optimum coupling were used. For the remaining lasers, the 10% output coupling mirror used was nearly optimum.

For S.Q.-1 and 2, a gas return pipe was used between the anode and cathode. This feature was not included in the remaining tubes. We have not yet been able to verify that the gas return feature offers any advantage in either power output or in tube life.

In all cases, the cathode used was of the reentrant type. Figures 4-5a and b show the design used for these experiments. On S.Q.-1 and 2, the cathode structure was directly exposed so that accurate temperature measurements could be made. On the remaining tubes, the cathode temperature could only be inferred.

TABLE 4-1

Construction Characteristics of Life Test Lasers Numbers

S.Q.-1 and S.Q.-2

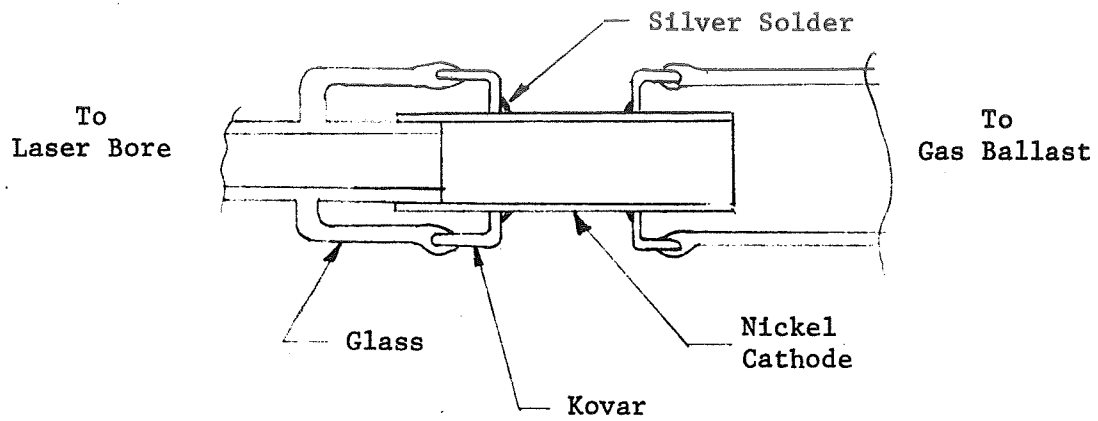
Active Length - - - - -	14 inches
Total Length - - - - -	17 inches
Mirror Configuration - - - - -	Flat Germanium etalon output, 3 meter radius of curvature gold coated non-output mirror. Internal mirror con- figuration.
Bore Diameter - - - - -	5.5 mm
Gas Storage Volume - - - - -	400 cc
Electrode Configuration - - - - -	Single anode and cathode
Tube Materials:	
Bore - - - - -	quartz
Storage Volume - - - - -	Pyrex
Cathode - - - - -	Nickel
Anode - - - - -	Gold Plated Tungsten
Optimum Current - - - - -	Approximately 8 mA at 8.2 kV tube voltage
Initial Power Output - - - - -	3-4 watts

TABLE 4-2

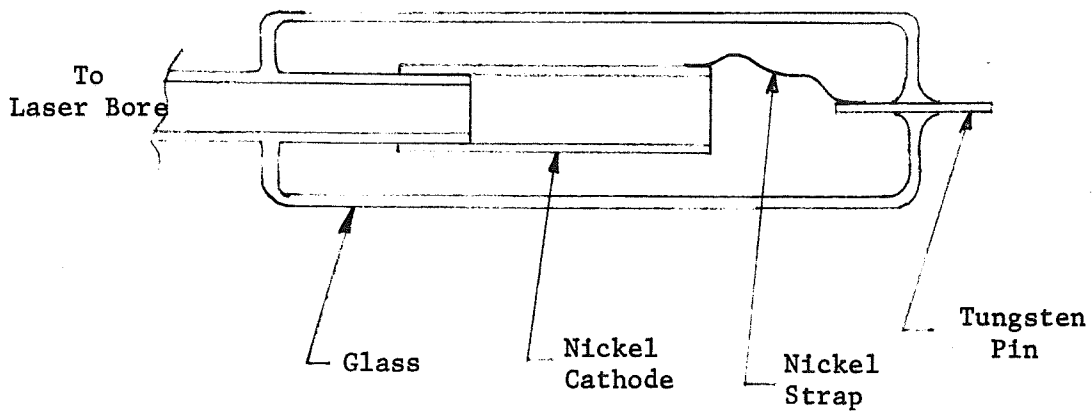
Construction Characteristics of Life Test Lasers Numbers

S.Q.-3, S.Q.-4, S.Q.-5

Active Length - - - - -	9 inches
Total Length - - - - -	13 inches
Mirror Configuration - - - - -	Flat 10% transmitting Germanium substrate, 60 cm radius of curvature gold coated non-output mirror, internal mirror configuration
Bore Diameter - - - - -	4.5 mm
Gas Storage Volume - - - - -	300 cc
Electrode Configuration - - - - -	designed to operate single cathode with one or two anodes
Tube Materials:	
Bore - - - - -	Pyrex
Storage Volume - - - - -	Pyrex
Cathode - - - - -	Nickel
Anode - - - - -	Gold Plated Tungsten
Optimum Current - - - - -	7 mA
Initial Power Output - - - - -	2-3.5 watts



a)



b)

Figure 4-5. Cathode Configuration for Life Test Lasers.

4.2.4 Life Test Results

S.Q.-1

This tube utilized a gas mixture of 0.1 torr H₂, 1.5 torr Xe, 1.8 torr N₂, 5.5 torr CO₂ and 12.0 torr He. It was operated at a current of about 7.0 mA and had a power output of about 2.8 watts.

The tube operated for approximately 550 hours with no change in power output or discharge characteristics, at which time the power output started to drop rapidly. After 587 hours the power output had dropped to near zero and was accompanied by a slight reduction in the voltage. Gas analysis on the tube indicated essentially no change in the relative pressures of the gas mixture from the original filling. Data on any possible change in total gas pressure could not be obtained with this tube.

The tube was dis-assembled and the cathode was cut apart for examination. A small shallow hole had developed in the cathode which appeared to be responsible for a large amount of local sputtering. If the sputtering caused a uniform reduction in gas pressure, it would explain the drop in tube voltage which occurred near the end of the life test.

S.Q.-2

This tube utilized an initial mixture of 1.5 torr Xe, 2.0 torr N₂, 6.0 torr CO₂ and 12.0 torr He. Prior to filling the tube, the cathode was pre-oxidized by operating the discharge in an oxygen atmosphere for about 15 minutes. A substantial amount of sputtering was noticed on the glass walls near the cathode at the conclusion of the oxidizing process. The tube was then filled and removed from the processing station and operated for about 600 hours before any gas samples could be taken. During this period no cathode heater was used.

The first gas analysis showed significant amounts of H₂ present in the discharge. Since the tube was only baked to 100°C during processing the hydrogen may have come from the tube walls in the form of water vapor.

Figure 4-6 shows the life history of this tube. During the first 600 hours, the laser operated with an unstable cathode discharge; that is, the emission region in the cathode wandered around the inside of the reentrant structure. During the next 700 hours, the cathode discharge stabilized and operated in one position, much smaller than the inside area of the cathode. During this period the power output dropped monotonically. At 1300 hours, the discharge appeared to jump every few days to a new position and the power output leveled off to a consistent value at about 30% of its initial figure. At 1700 hours the cathode was heated briefly and the tube appeared to rejuvenate. The increase in output power was short lived, however. It appeared that the cathode must be continuously heated. These results follow closely those found by Deutsch and Horrigan.⁽¹⁰⁾ At 1900 hours the cathode was heated continuously and the power rose to 89% of its original value. After heating the cathode continuously, the cathode discharge again became unstable in location and has remained unstable to the present time. Recently the cathode temperature was increased by 20°C and a small but short-lived rise in output power occurred.

During this entire period the discharge voltage at a fixed operating current of 8.2 mA has remained at 8.2 ± 0.1 kV.

This tube shown in Figure 4-7 is equipped with a Granville-Phillips variable leak valve rather than a calibrated gas sampling valve, so no record of total gas pressure variations is available. Consistent gas analysis data were not available until after the tube had operated for nearly 2000 hours. Since that time essentially no change in gas composition has occurred except for a slight reduction in the amount of H₂ and H₂O.

During the period of lower power operation, the current for optimum power output dropped from an original value of 8.2 mA to about 5 mA at the lowest power levels. Although the laser power dropped by a factor of about 3, the overall laser efficiency (including ballast



Figure 4-7. Life Test Laser, S.Q.-2.

resistors) only dropped by a factor 1.5. Although the optimum current is again back to its original value, it appears that a step control feature for the laser current and may indeed prolong the useful life of the CO₂ laser.

During the thermal rejuvenation process for the laser, an effort was made to determine the minimum cathode temperature which would rejuvenate the SQ-2 laser. With the cathode at 110°C, the output power was at its lowest level (1 watt). Wrapping the cathode with insulation raised the temperature to 160°C but only raised the power output to about 1.2 watts. At 250°C, the power output slowly rose to about 2.5 watts over a period of several days. An increase to 280°C resulted in a rapid power increase to 2.9 watts, where it leveled off. It appears that cathode temperatures somewhat above 250°C will be necessary.

At the writing of this report the SQ-2 laser has now operated for 3400 hours and is presently at 78% of its original power. It is still premature to predict whether the goal of 10,000 hours at the 40% power level will be achieved with this tube; however, it appears that the technique of using H₂ in the gas mixture along with a properly-designed heated Nickel cathode will eventually allow attainment of this figure.

S.Q.-3

This laser was the first of the shorter variety with a more optimally designed optical cavity. The gas mixture used with this tube was 0.25 torr H₂, 0.5 torr Xe, 7.0 torr N₂, 9.0 torr CO₂ and 20.0 torr He. The laser emitted approximately 2.7 watts at seal-off. This tube, shown in Figure 4-8, used a single cathode and single anode and operated at a tube voltage of about 5.7 kV with an optimum current of 7 mA. The cathode was heated to approximately 280°C from the start.

Figure 4-9 shows the history of this tube. The power output of the laser slowly increased throughout the life test on the tube until a

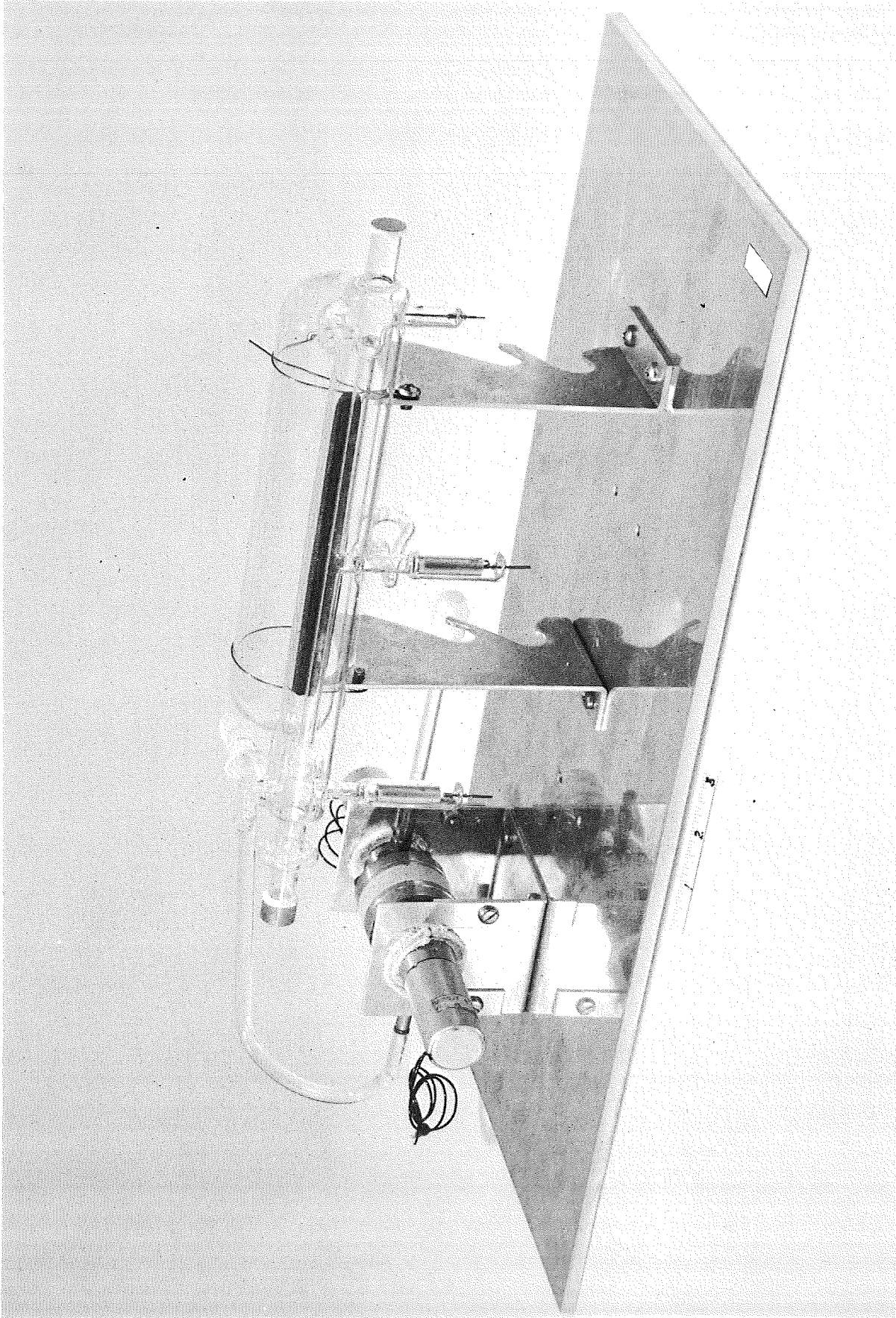


Figure 4-8. Life Test Laser, S.Q.-3.

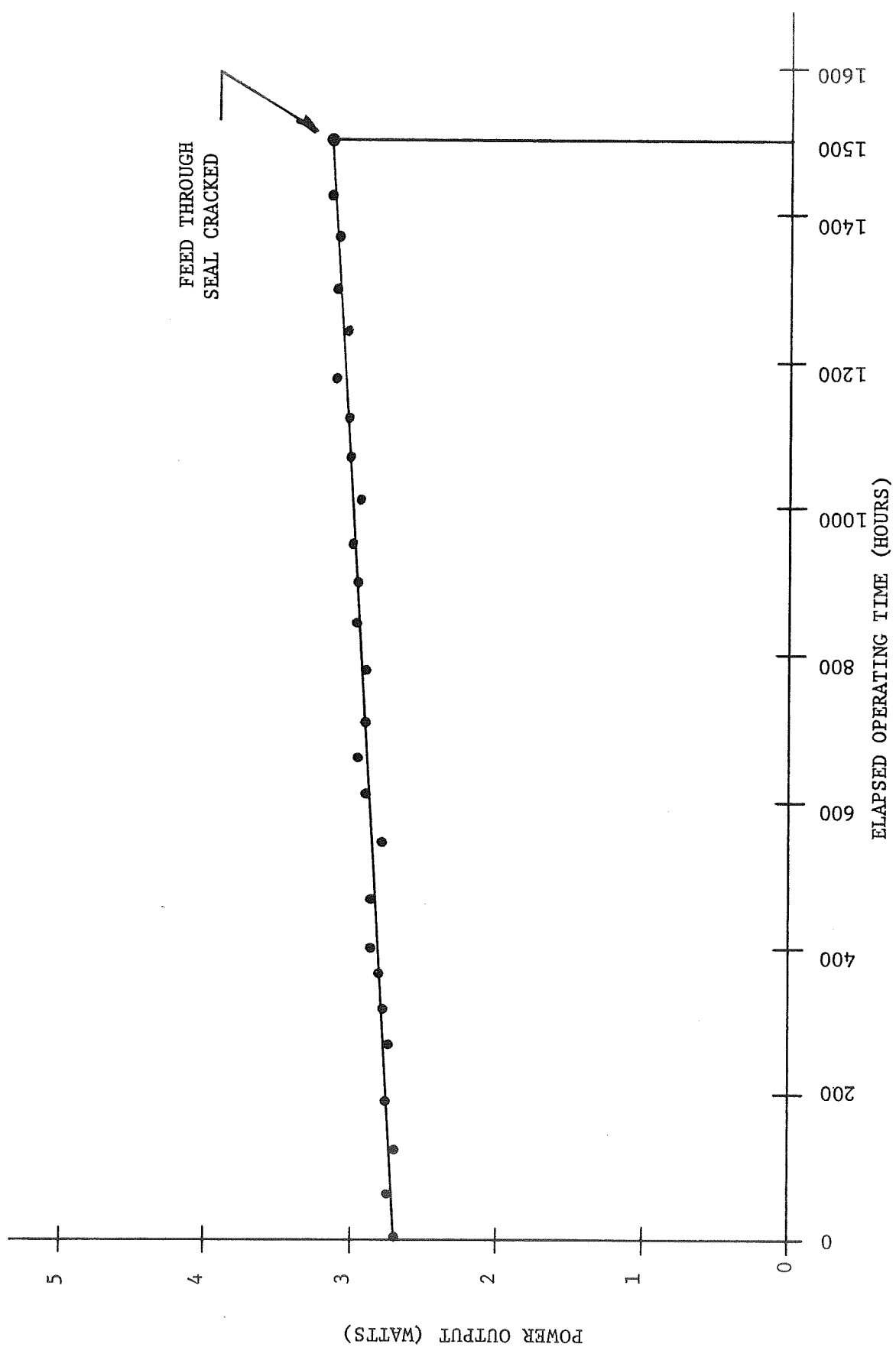


Figure 4-9 Life History of SQ-3 Laser Cathode Heated From Start of Life Test

crack developed in the cathode feed through pin. This unfortunate occurrence concluded what appeared to be the best run of all the tubes to be tested to date.

In this tube the cathode was designed with a slightly smaller internal diameter (.320 inch) than used with the S.Q.-2 laser. As a result, the discharge covered the inside surface of the cathode quite uniformly and no discharge instability was observed.

S.Q.-4

This tube was identical to S.Q.-3 except that it used two anodes and a heated central cathode. It was intended to show if operating lifetime is affected by higher cathode current operation. After approximately 100 hours of operation, a leak developed (again at the cathode feed-through seal), ending the test.

S.Q.-5

This was the first tube to operate with the sampling valves. After about 250 hours of operation it, too, suffered a crack at the cathode feed-through seal. Apparently a chemical change is taking place in the glass next to the tungsten feed-through even though the temperature rise is not extreme because of the increased cathode temperature. The seal becomes strained and cracks within only a relatively few hours. Many other identical seals in unheated structures have lasted for years. The cathode structures on the remaining life test lasers are being redesigned to remove this problem.

The S.Q.-3, 4, 5 tubes mentioned above are being reworked, using the new cathode design. Several more lasers are now being processed and will be operated on life tests during the next phase of the program. Ceramic tube structures will also be placed on life test during the next phase.

4.3 GaAs Window Sealing Studies

A number of low vapor pressure epoxies have been used to seal GaAs windows to CO₂ laser tubes. These seals have been generally satisfactory, but have a number of disadvantages when considered for use in space. The epoxy seals occasionally fail through poor adhesion to the GaAs windows, and it is difficult to determine in a particular case whether the adhesion is good.

In addition, the thermal expansion coefficients of the epoxy and the GaAs are not well matched, leading to concern about the effect of repeated thermal cycling on the seal. Finally, we wish to avoid the use of organic compounds in space in order to obtain the longest possible life. We have therefore developed an all-metal seal for the GaAs windows which is reliable and strong and which withstands thermal shock well. The general technique is to gold plate the end of a metal tube and a matching ring on the GaAs window. The window is then pressed against the tube and heated in a reducing atmosphere to a temperature which causes the Au to alloy into the GaAs, thus bonding the GaAs to the metal tube. The window bonds so formed have been mechanically strong but not necessarily vacuum tight. To insure a vacuum seal, a fillet of soft solder is then formed on the outside of the metal to GaAs joint. Windows sealed in this manner have been subjected to repeated thermal shock by plunging them first into liquid nitrogen (77°K) and then into water (300°K) without fracture. The seals show no leaks on a 1×10^{-10} STD cc/sec leak detector.

The linear expansion coefficient of GaAs is $(6.86 \pm 0.13) \times 10^{-6} \text{ (}^\circ\text{C)}^{-1}$ between -62°C and 200°C ⁽¹¹⁾. Of the commonly available metals which might be used in forming a seal to GaAs, Mo and Kovar most nearly match this expansion coefficient. The linear expansion coefficient of both these metals is approximately $5 \times 10^{-6} \text{ (}^\circ\text{C)}^{-1}$.⁽¹²⁾ Mo is commonly used as a contact metal for GaAs in the semiconductor industry and for that reason was tried first. Tests with Kovar are presently being conducted. In the final tube Kovar will be used, primarily because it can be heliarc welded. After the GaAs window is sealed to a short section of Kovar tubing, the Kovar will in turn be heliarc welded to the laser tube.

Short pieces of Mo tubing were gold plated and hydrogen fired. A matching ring of gold was evaporated on a polished semi-insulating GaAs window. The tubing was then pressed against the GaAs window and the assembly was heated in hydrogen to a temperature slightly above 450°C, the temperature at which Au alloys into GaAs. In most cases, the window was fused to the metal tube by this operation in a joint which is mechanically strong and which withstood thermal shock well. When the window was knocked off forcibly the failure was in the GaAs, pieces of which pulled out of the window and remained on the metal tube. Our original intention was that this Au alloy seal would be sufficient. We found, however, that with the joining pressures used (a few hundred gm/cm², the joint was not vacuum tight. We have therefore plated the joint with Ni, and formed a fillet of relatively soft solder around it to provide the vacuum seal. The resulting seals have been found to be entirely satisfactory. Figure 4-10 shows one of the completed test pieces. In future work the joining pressure will be increased, and more care will be taken to obtain flat joining surfaces in order to obtain as strong an alloy seal as possible. At this point, however, the addition of a soft solder fillet appears to provide at the least an added safety margin on bond strength, and its use will be continued.

Finally, the transmission of the GaAs windows used in these tests has been checked before and after the heat treatment used to alloy the gold to the surface, and no change in transmission has been observed.

In summary, an all metal seal has been developed for the GaAs CO₂ laser windows which is mechanically strong, resistant to thermal stress, vacuum tight, and which does not affect the optical properties of the window.



Figure 4-10. Gallium Arsenide Window Sealed to Molybdenum Tubing by Metal Soldering.

4.4 Beryllium Oxide Leak Rate Measurements

Beryllium oxide is a pressed and sintered ceramic made from the powdered form. The properties of the material are grossly affected by the material density and impurity composition. Also, some researchers have claimed that the material may be rather porous to gas, and may not make a reliable vacuum envelope for the space qualified laser.

Although BeO is used extensively as an ultra-high vacuum dielectric material in the tube industry, it has rarely been used as a vacuum envelope, primarily because of its high relative cost compared to aluminum oxide ceramic. Therefore, few data are available on the leak rate characteristics of the material. A series of experiments on several samples was conducted during this program to determine if the porosity of the material would be a problem in this application.

4.4.1 Tube Leak Rate Requirement

The desired sealed-off lifetime of the S.Q. laser is given as 3 years. Therefore, in the vacuum environment of space, the laser must not lose a significant amount of gas during this period by pumping through the tube envelope. As a criterion for evaluation, we have set a requirement that the laser tube should not lose more than about 1 torr of helium during the 3 year period. This represents about a 10 percent reduction in helium tube pressure, which will not significantly change the tube operating characteristics. Since helium has a substantially higher leak rate through porous structures than the other gases used in the laser, the partial pressures of the other gases will be much less affected.

We can now calculate the maximum tolerable leak rate through the walls of the laser tube.

Let P designate the pressure in the volume, V, of the laser tube at any time during the period. The rate of gas removal, assuming the external pressure is small compared to P, is approximated by

$$P = P_0 e^{-tC/V}$$

where C is the gas conductance of the tube walls in cc/sec, and P_0 is the initial helium pressure. Then,

$$\frac{dP}{dt} = -\frac{P_0 C}{V} e^{-tC/V}$$

At time near zero the rate of pressure drop can be estimated by

$$\frac{\Delta P}{\Delta t} = -\frac{P_0 C}{V}$$

For our case

$$\begin{aligned} \Delta P &= -1 \text{ torr} \\ \Delta t &= 3 \text{ years} \approx 10^8 \text{ sec} \\ P_0 &= 10 \text{ torr} \\ V &= 150 \text{ cc.} \end{aligned}$$

Therefore the total conductance of the BeO material must be less than

$$C \leq 1.5 \times 10^{-7} \text{ cc/sec,}$$

assuming that no other tube materials have significant leak rates.

The area of the BeO which is expected to be exposed to the vacuum environment is about 25 cm^2 . Therefore the average conductance per unit area, \bar{C} , should be

$$\boxed{\bar{C} \leq 6 \times 10^{-9} \text{ cc/sec/cm}^2} \quad \text{leak out of tube}$$

Also of importance is the leak rate into the tube as the tube is stored on the ground at atmospheric pressure. The appropriate approximate equations describing this condition are:

$$P = P_a - (P_a - P_0)e^{-tC/V}$$

where P_a is atmospheric pressure outside the tube (760 torr). Then,

$$\frac{\Delta P}{\Delta t} = (P_a - P_0) \frac{C}{V} e^{-tC/V}.$$

For the same conditions as above, the requirements on the leak rate are:

$$\boxed{\bar{C} \leq 8 \times 10^{-11} \text{ cc/sec/cm}^2} \quad \text{leak into tube .}$$

4.4.2 BeO Leak Rate Experiments

Several cylindrically shaped samples of BeO were leak checked on a calibrated VEECO He mass spectrometer with a sensitivity of better than 2×10^{-10} ATM cc/sec. One end of the cylinder was sealed with "Torr-Seal" epoxy and the other attached to the leak detector. None of the samples showed an indication of a leak when probed with a small stream of helium. A glass enclosure was then used to cover the BeO tube. The region between the glass tube and the BeO was filled with helium gas after which the tube was sealed.

Table 4-3 shows the results of the tests. In all cases, a leak could be detected, although approximately two hours were required before the measured leak rate reached equilibrium.

The measured leak rate, R , is related to the conductance by

$$R = \Delta P_a C$$

where ΔP_a is the pressure difference across the sample being tested. In our case, $\Delta P_a = 760 \text{ torr} = 1 \text{ ATM}$.

Both samples 1 and 2 were obtained from Brush Beryllium Corp. and are not necessarily their highest density material.

Table 4-3.
Measured Leak Rates and Corresponding
Conductance on Beryllium Oxide Samples.

Sample	1	2	3
Size	$\frac{3}{8}$ " OD x $\frac{1}{4}$ " ID x 10" long	$\frac{3}{8}$ " OD x $\frac{1}{8}$ " ID x $8\frac{5}{8}$ " long	Same as 2
Surface Area	76 cm ²	66 cm ²	66 cm ²
He Leak Rate, \bar{R} , at atmos- pheric pressure (ATM cc/sec/cm ²)	4.8×10^{-10}	1.8×10^{-10}	7.0×10^{-11}
Corresponding Conductance (cc/sec/cm ²)	4.8×10^{-10}	1.8×10^{-10}	7.0×10^{-11}

Sample 3 and 2 used the same BeO material; however, 3 was coated with a thin film of "Vac-Seal," a high vacuum silicone sealant. As can be seen, a marked reduction in the leak rate was obtained, although the thin film did not completely seal the BeO.

The results obtained with sample No. 3 show that the desired porosity level can be achieved, however, it would be much preferred if the additional sealing requirement were not needed.

More samples of high density BeO material which are especially processed for high vacuum work will be obtained for future tests. Also, all of the BeO purchased for use in the mock-up and final ceramic tubes will be tested for porosity since characteristics can vary from piece to piece.

4.5 Mock-up Laser Tests

A GaAs Brewster angle laser tube was constructed with an active length and bore diameter closely approximating that proposed for the ceramic space qualified laser. The bore size for this laser was 4 mm. It was constructed from quartz. As shown in Figure 4-11, the electrodes were, for convenience, placed in side tubes rather than coaxially. It used a center cathode and two anodes and had an active length of 16.6 cm. The total length of the tube was 26 cm. The power output characteristics of this tube should closely approximate that expected from the final design; however, the efficiency will be somewhat lower because of the greater electrode separation.

A series of parametric tests were run to determine the optimum gas mixture. With a five gas mixture, it is almost impossible to determine the optimum mix; however, the following mixture gave the best results:

H ₂ :	0.15 torr	
Xe:	0.3	
N ₂ :	5.0	Total Pressure = 23 1/2 torr
CO ₂ :	5.0	
He:	13 torr	

The peak power output was 2.1 watts, single-mode with a 5% transmission output mirror and a 47 cm radius of curvature gold mirror. At the maximum power output, the tube voltage was 3.4 kV and the tube current was 8 mA/leg. The tube efficiency was 4.2%.

At a current of 3 mA per leg, the tube voltage was 3.0 kV and the power output was 0.9 watts, giving a tube efficiency of 5.0%. Extrapolating these results to the case of a tube with coaxial geometry, in which approximately 5 cm of discharge length per leg can be eliminated, the tube efficiency should be 7.3% at the operating current of 3.0 mA. The tube voltage should be about 2100 V.

It is felt that further optimization is still possible; this will be examined in the next phase. Tube efficiency of 9-10% may indeed be feasible in this small size, even with the relatively large fixed losses in the laser optics and in the electrodes.

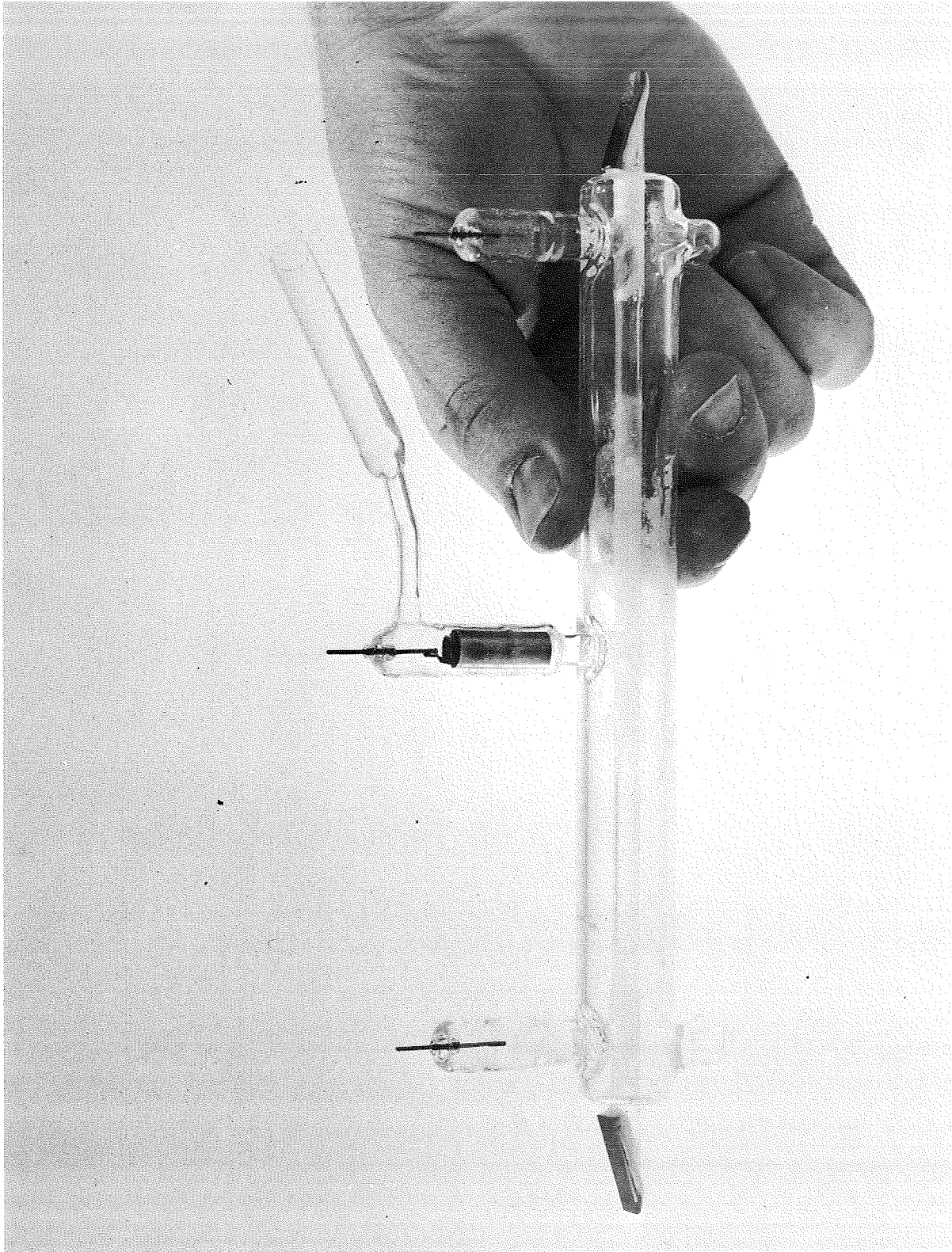


Figure 4-11. Test Laser Used to Evaluate the Properties of the Space Qualified Laser Design

A second mock-up tube, shown in Figure 4-12, was completed just prior to the writing of this report. It features a coaxial electrode design in order to verify the voltage and current predictions given earlier. Although the tube has not yet been operated as a laser, its discharge characteristics for the above laser mixture have been measured. The required tube voltage as a function of current per leg is shown in figure 4-13. Here we see that the required tube voltage at the expected operating current of 3 mA per leg is 1810 volts, somewhat less than originally expected.

4.6 Electrode Fall Studies

In any discharge tube, there exists a power loss associated with the cathode fall and anode fall. This power, which is dissipated in the electrodes, is essentially independent of tube length and, as a result, is an important limiting parameter on the maximum efficiency which can be obtained from short laser tubes.

Some tests were run on several types of possible cathode materials in an attempt to determine approximate electrode fall voltages. This information can then be used to help determine the maximum possible efficiency which can be expected from the S.Q. CO₂ laser. For our purposes, the electrode fall is the lowest voltage which can be applied to a discharge tube in order to maintain a stable discharge as the electrode spacing is reduced to zero.

Several discharge tubes similar to that shown in Figure 4-14 were constructed. For a typical CO₂ lasing mixture, the voltage between the cathode and one of the two anodes was taken as a function of current. The same data was then taken for the second anode. As an approximation, the voltage drop per unit length along the discharge can be considered constant since the major portion of the discharge is operating in the positive column. By extrapolating the data to zero electrode spacing, the electrode fall voltage can be obtained.

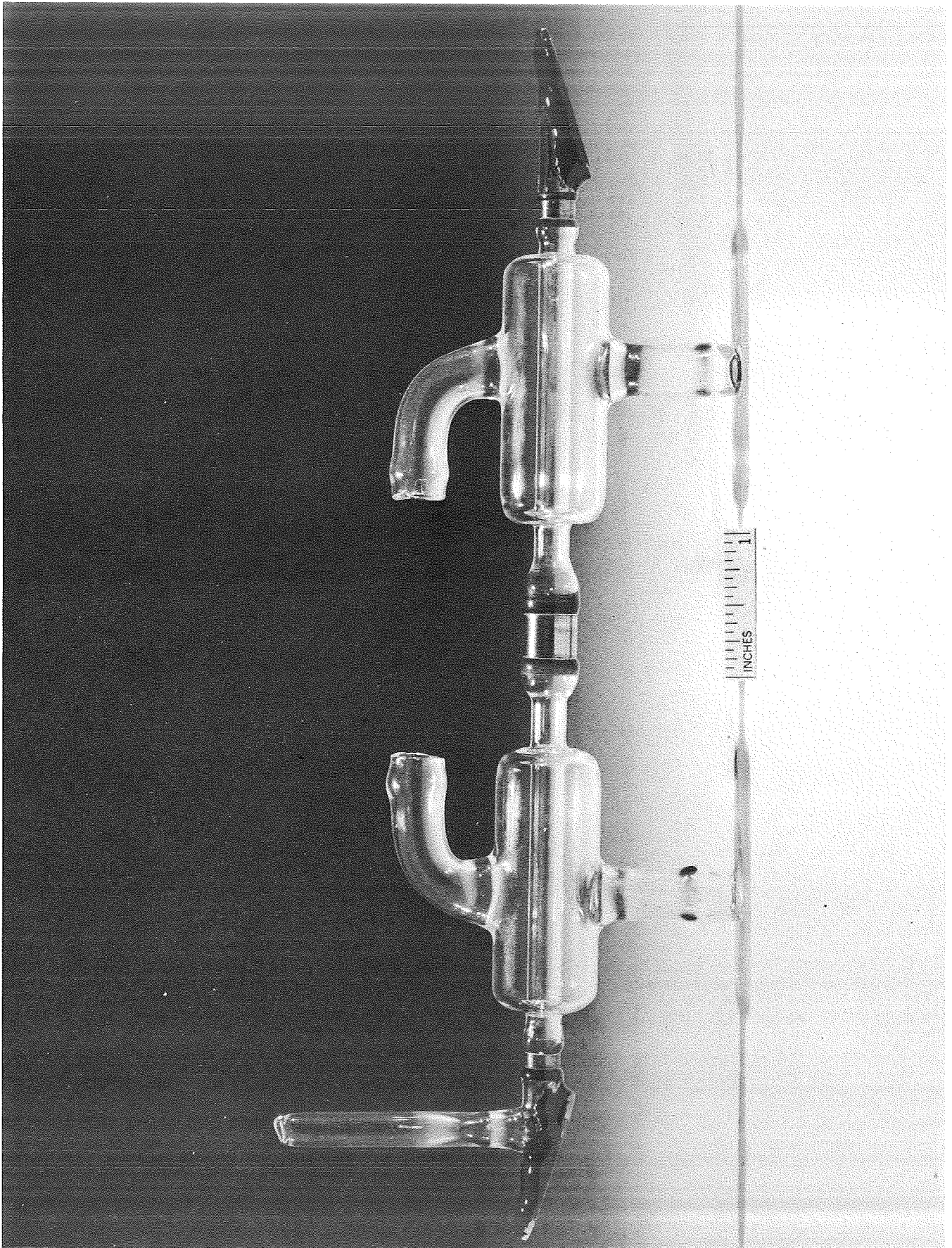


Figure 4-12. Test Laser with Coaxial Electrodes.

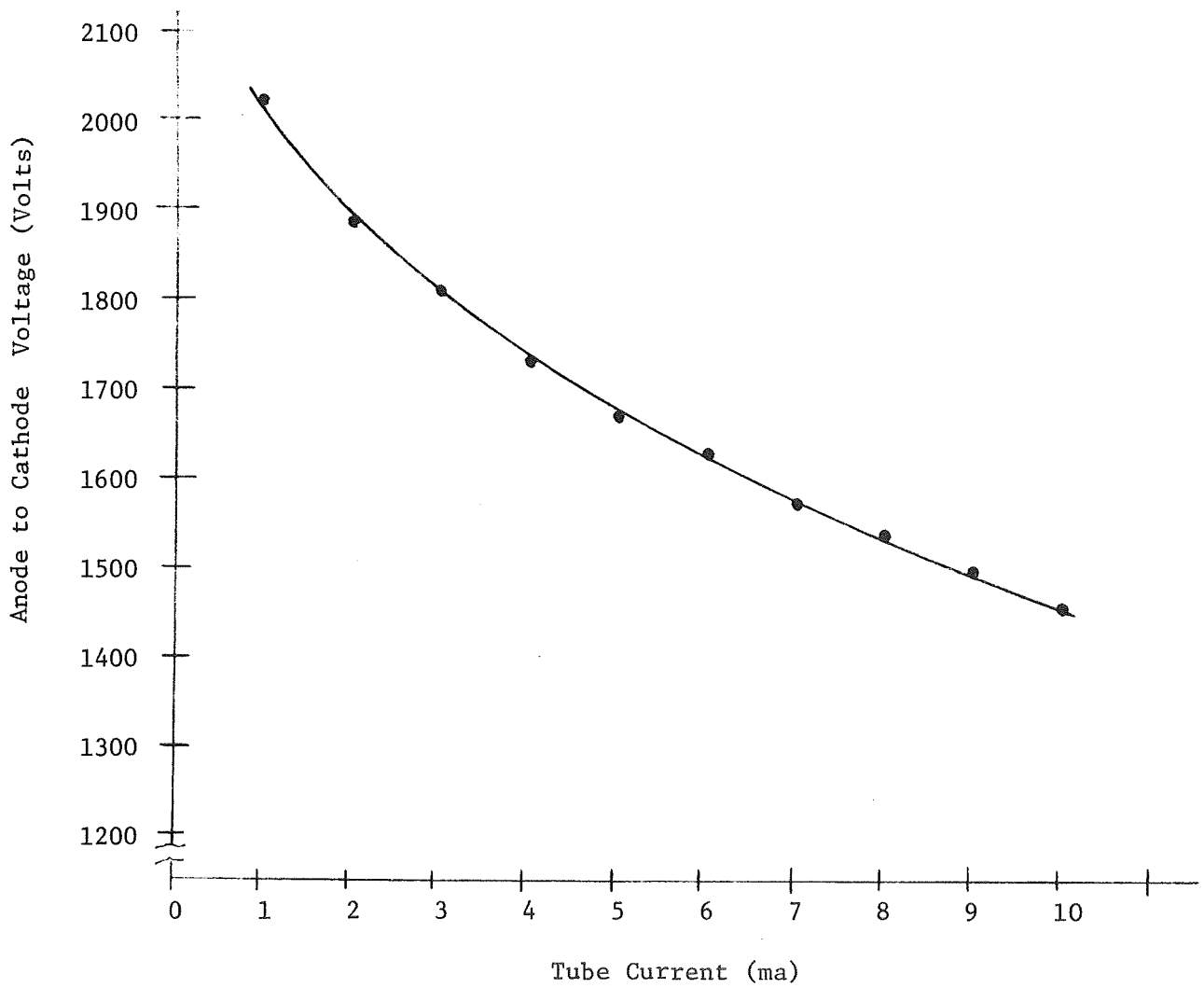


Figure 4-13. Voltage-Current Characteristics of Coaxial Mock-up Laser Tube

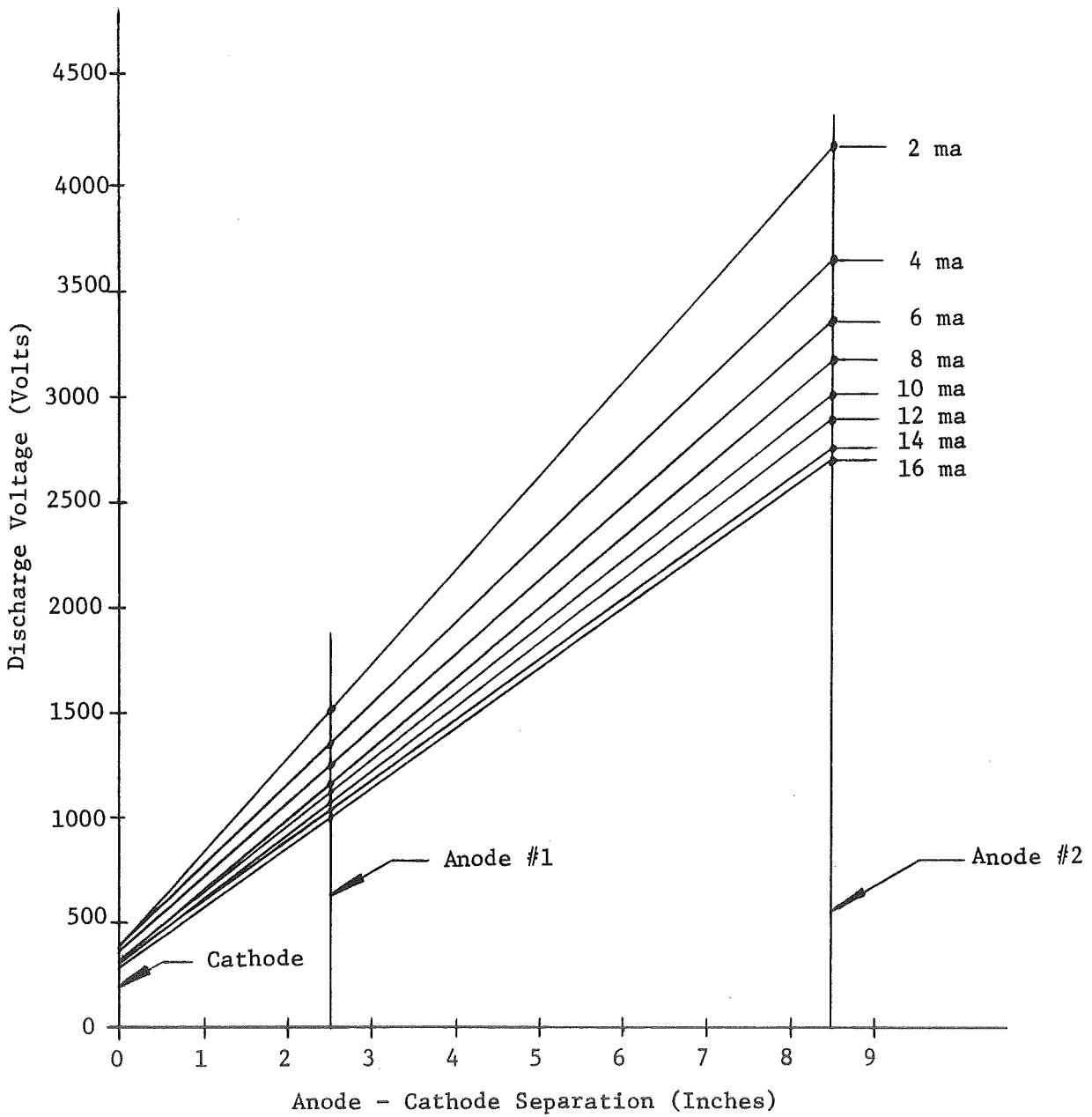
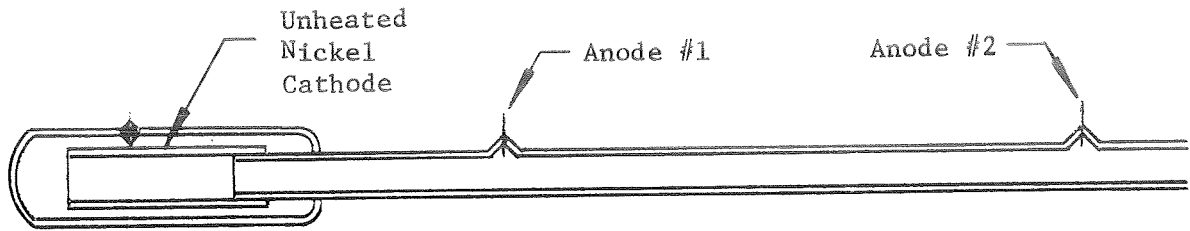


Figure 4-14. Extrapolation of Discharge Characteristics to Determine Electrode Fall.

As depicted in Figure 4-14, the electrode fall for a pure Nickel cathode ranges between about 270 and 350 volts depending on the discharge current. Comparative results were obtained for several other potential cathode materials and the results of these tests are shown in Table 4-4.

TABLE 4-4

Approximate Electrode Fall Voltages for
Several CO₂ Laser Cathode Materials

<u>Material</u>	<u>Electrode Fall (Volts)</u>
Pure Nickel	300
Nickel - Gold Alloy #1	290
Nickel - Gold Alloy #2	320
Kovar	280
Platinum	630

The Nickel, Kovar and Platinum electrodes were studied since all three have been used fairly extensively as CO₂ laser cathode materials. The Nickel-Gold alloys may have an advantage by providing a catalytic agent (Gold) to increase the recombination rate of CO and oxygen to form CO₂, while still maintaining the advantage of emission from a nickel oxide surface. This catalytic effect with relatively cold platinum or gold was first described by Lawrence⁽¹³⁾.

The Ni-Au alloy cathodes were formed by plating a pure nickel tube with varying thicknesses of gold. Alloy #1 was plated with .0001 inch of gold, while alloy #2 was plated with .001 inch of gold. The plated cathodes were then heated in a hydrogen atmosphere to 600°C for 6 hours to form the alloy. The results on these cathodes show that presence of a small amount of gold in the nickel does not have a major effect on the electrode fall characteristics. It did appear, however, the discharge area was increased slightly over a pure nickel cathode. The cathodes were operated continuously for several days to see if the alloys exhibited significant sputtering. No sputtered material on nearby glass was observed for the pure

nickel and alloy #1 but evidence of very slight sputtering was seen with alloy #2.

The platinum cathode demonstrated a definitely higher electrode fall figure and accounts in part for its observed higher sputtering rate.

The electrode fall data were also taken for several gas mixtures appropriate for CO₂ lasers. Within the experimental error, no difference was seen in the electrode fall voltages.

For the expected cathode currents (6 mA total), the power lost in the electrodes would be about 1.8 watts for the Nickel materials and about 3.8 watts for a platinum electrode. These figures are significant compared to the total expected tube powers of about 13 watts, and point out the desirability of not using platinum.

5.0

MATERIALS LIST

The following is a list of materials expected to be used in the space qualified CO₂ laser.

Beryllium Oxide Ceramic
Aluminum Oxide Ceramic
Kovar
Gallium Arsenide
Gold
Nickel
Indium Solder
Stainless Steel
Aluminum
Fuzed Quartz
Lead-Zirconium-titanate ceramic
Gold-copper Braze Alloy
Gases: CO₂, He, N₂, Xe, H₂
Torr Seal Epoxy
Lead-Tin Solder
Potting Material
Electrical Components

6.0 SUMMARY AND CONCLUSIONS

The preliminary design for a space qualified 1 watt single-frequency CO₂ laser was completed, resulting in a laser package with dimensions of 4" x 4" x 12" and weighing 5.9 lbs. exclusive of power supply. The power supply, which is an external package, has dimensions of 2" x 4" x 9" and weighs 4.2 lbs. The prime power requirement will be less than 20 watts for normal operation. An auxiliary electronic frequency control unit which may be added to the laser as an accessory will have dimensions of about 1" x 2" x 4" and will weight 0.8 lbs. It will require about 1 watt of prime power.

The laser tube utilizes metal-ceramic construction techniques for rigidity and reliability. The laser is cooled by conduction to the space craft heat sink. Gallium arsenide Brewster windows are used to obtain a polarized output. Two inches of open space within the laser cavity are available if the addition of a modulator is required at a later date.

To verify the feasibility of the design and to determine the values of many of the design parameters, a series of experimental studies was pursued during the program. Life test studies on glass-envelope lasers has indicated that a laser which utilizes a heated nickel cathode and a gas mixture of H₂, Xe, CO₂, N₂ and He may be capable of providing the desired operating lifetime of 10,000 hours. One laser still on life test has operated for over 3400 hours and is still above 75% of the original output power.

An ultra-high-vacuum metal soldering technique was developed for the attachment of gallium arsenide windows to metal substrates, replacing epoxy joints now used. The technique should allow temperature cycling of the gallium arsenide window from at least -196°C to +200°C, although tests to date have only been performed between -196°C and 20°C.

Tests on mock-up lasers have indicated that to achieve maximum efficiency from the laser, a coaxial electrode design should be used. Cathode fall studies on various possible cathode materials have shown that approximately

2 watts of electrical power not useable for laser action will be dissipated in the tube electrodes if a nickel cathode is used. Platinum cathodes would exhibit almost twice this power loss.

The power supply to be used with the laser will be capable of an output voltage of 3.5 kV continuous with 5 kV laser starting pulses, and will use active current regulation. The supply will also be capable of step-wise current set so that optimization of the laser output power will be possible throughout its useful life. The power supply will have an overall efficiency of about 80%.

The experimental tests have definitely shown that the desired specifications are feasible with the proposed design and that breadboarding of the laser should be started in the next phase (Phase II) of the contract.

- (1) C. G. B. Garrett, GAS LASERS, Pg. 35 McGraw-Hill, New York, 1967.
- (2) J. H. McElroy and H. E. Walker, "Laser Mirror Transmissivity Optimization in High Power Optical Cavities," to be published.
- (3) T. Li, "Diffraction Loss and Selection of Modes in Maser Resonators with Circular Mirrors," B.S.T.J., 45, 917 (May 1965).
- (4) C. Freed, "Design and Short-term Frequency Stability of Single-Frequency CO₂ Lasers," IEEE Jour. Quantum Electronics, QE-4, 404 (June 1968).
- (5) M. W. Sasnett, et al., "10.6 Micron Laser Frequency Control Techniques," Technical Report AFAL-TR-68-210, September 1968.
- (6) M. W. Mocker, "Pressure and Current Dependent Shifts in the Frequency of Oscillation of the CO₂ Laser," Appl. Phys. Lett 12, 20-23, 1 January 1968.
- (7) M. W. Sasnett, "10.6 Micron Laser Frequency Control Techniques," Technical Interim Report on Contract F 33615-69-C-1182, 28 July 1969, Sylvania Electronic Systems, Mountain View, California.
- (8) J. M. Meek and J. D. Craggs, Electrical Breakdown of Gases, (Oxford Press, London, 1953)
- (9) R. J. Carbone, "Continuous Operation of a Long-Lived CO₂ Laser Tube," JQE, QE-4, 102 (March 1968).
- (10) T. F. Deutsch and F. A. Horrigan, "Life and Parameter Studies on Sealed CO₂ Lasers" IEEE Jour. Quantum Electronics, QE-4, 972 (November 1968)
- (11) E. D. Pierrun et. al., JAP 38, 4669, (1967)
- (12) ASM Metals Handbook, 8th Ed. Vol. 1
- (13) T. R. Lawrence, "Chemical Reactions of Gases in Electrical Discharges", paper presented at the 2nd Conference on Chemical and Molecular Lasers, St. Louis, Mo., May 22-24, 1969.
- (14) M. Born and E. Wolf, Principles of Optics, (MacMillan, N. Y., 1964), pg. 325.

APPENDIX A

New Technology

Low Temperature Metal Soldering Technique for Gallium Arsenide Optical Windows

Metalizing techniques have previously been developed for Gallium Arsenide in the semiconductor device industry. During this program, these techniques have been utilized to develop a procedure by which high resistivity Gallium Arsenide optical windows can be soldered to a metal structure without destroying their optical quality. The metal seals which are made by this process withstand thermal shock and are vacuum tight.

Section 4.3 of this report details the technique developed.